Food Research International 157 (2022) 111270

Contents lists available at ScienceDirect

Food Research International

journal homepage: www.elsevier.com/locate/foodres

Contribution of the proximal and distal gastric phases to the breakdown of cooked starch-rich solid foods during static *in vitro* gastric digestion

Joanna Nadia [a,b], John E. Bronlund [a,b], Harjinder Singh [a], R. Paul Singh [a,c], Gail M. Bornhorst [a,c,*]

[a] Riddet Institute, Massey University, Private Bag 11222, Palmerston North 4442, New Zealand
[b] School of Food and Advanced Technology, Massey University, Private Bag 11222, Palmerston North 4442, New Zealand
[c] Department of Biological and Agricultural Engineering, University of California, Davis, CA 95618, USA

ARTICLE INFO

Keywords:
Amylolysis
Acid hydrolysis
Biochemical breakdown
In vitro gastric digestion
Physical breakdown
Starch

ABSTRACT

In vitro gastric digestion studies commonly focus on the acidic environment of the stomach (the distal phase), neglecting that the contact time between food and salivary amylase can be extended during bolus' temporary storage in the proximal stomach (the proximal phase). Consequently, the role of the proximal phase of gastric digestion on the breakdown of solid starch-based foods is not well understood. This study aimed to address this question using a static *in vitro* digestion approach. Cooked starch-rich foods of different physical structures (wheat couscous, wheat pasta, rice couscous, rice noodle, and rice grain) were subjected to 30 s oral phase digestion, followed by prolonged incubation of the oral phase mixture (pH 7) for up to 30 min representing different proximal phase digestion times. Each proximal phase sample was sequentially incubated in excess simulated gastric fluid (distal phase, pH 2) for up to an additional 180 min. The proximal phase aided solid food breakdown through starch hydrolysis that caused leaching of particles <2 mm. The distal phase led to softening of food particles, but the softening process was not enhanced with longer proximal phase. In foods with smaller initial size (couscous and rice couscous), a proximal phase of 15 min or longer followed by 180-min distal phase increased starch hydrolysis in the liquid and suspended solid fractions of the digesta, indicating the influence of food structure on acid hydrolysis during *in vitro* gastric digestion.

1. Introduction

Gastric digestion is important for the physical breakdown of solid foods in the gastrointestinal tract as it influences nutrient delivery to the small intestine. Particularly for starch-rich foods, gastric emptying rate is crucial to their glycemic response profile, which may be modified through food structuring to alter food breakdown rate in the stomach (Nadia, Bronlund, Singh, Singh, & Bornhorst, 2021). Despite its importance, the role of the stomach in the digestion of solid starch-rich foods is not well-understood – possibly due to the commonly accepted view that the stomach has an acidic environment (pH ≤3), which is inconducive for salivary amylase activity to biochemically digest the starch (Brownlee, Gill, Wilcox, Pearson, & Chater, 2018). Consequently, *in vitro* starch digestion procedures typically simulate the gastric digestion step at pH ≤3 with excess gastric fluid (Englyst, Englyst, Hudson, Cole, & Cummings, 1999; Goñi, Garcia-Alonso, & Saura-Calixto, 1997; Monro, Mishra, & Venn, 2010) and heavily focus on the small intestinal stage. Other non-starch specific *in vitro* methods that focus on biochemical changes during digestion, such as the INFOGEST static digestion protocol (Brodkorb et al., 2019; Minekus et al., 2014), proposed gastric digestion at pH 3.0 with limited amount of gastric fluid. These available procedures are generally conducted using ground samples, which eliminates the physical structure of the foods. However, the actual stomach consists of two physiological regions (proximal and distal) with different features and biochemical environment that may impact starch digestion.

After meal consumption, the proximal stomach serves as a temporary bolus storage with minimal contractions. The distal stomach acts as a grinder for mechanical breakdown of solid foods; it is the initial location for acidic gastric fluid accumulation, and it aids in mixing between the food bolus with gastric fluid through gastric peristaltic contractions. Previous *in vivo* studies, where growing pigs were fed with foods of varying composition and structures, reported higher intragastric pH in the proximal stomach compared to the distal stomach as a result of

* Corresponding author.
E-mail address: gbornhorst@ucdavis.edu (G.M. Bornhorst).

https://doi.org/10.1016/j.foodres.2022.111270
Received 21 February 2022; Received in revised form 15 April 2022; Accepted 17 April 2022
Available online 20 April 2022

gradual addition of gastric fluid, different rates of acidification of gastric content, and variations in meal mixing with gastric secretions (Bornhorst, Rutherfurd, et al., 2014; Nadia, Olenskyj, et al., 2021; Nau et al., 2019). These studies indicated that the intragastric pH may remain within the working pH range of salivary amylase (pH ≥3) for up to 1 h, allowing for extended salivary amylase action in the stomach.

Prolonged contact between active salivary amylase and ingested food has been reported to increase starch hydrolysis in *in vitro* studies using solid starch-based products (Freitas & Le Feunteun, 2019; Freitas, Le Feunteun, Panouille, & Souchon, 2018; Gao et al., 2021; Tagle-Freire, Mennah-Govela, & Bornhorst, 2022; Wu et al., 2017). Increased starch hydrolysis is also expected in the proximal stomach (proximal phase), which may subsequently affect the breakdown of food particles when digesta from the proximal stomach enters the distal stomach (distal phase) (Nadia, Olenskyj, et al., 2021). Physical changes of starch-rich foods during gastric digestion without the proximal phase (only considering the distal phase) have been previously studied *in vitro* (Drechsler & Bornhorst, 2018; Kong, Oztop, Singh, & McCarthy, 2011; Mennah-Govela & Bornhorst, 2016a; Somaratne et al., 2020). In these previous studies, it was found that physical changes of food particles (in the form of particle softening and/or solid loss over time) were related to the physical structure of the food resulting from different starch sources and cooking/processing methods. However, starch hydrolysis, which may impact the physical changes, was not measured. Additionally, how physical changes during the distal phase and the properties of particles emptied from the distal phase may be impacted by a prolonged proximal phase are not understood (Nadia, Bronlund, et al., 2021).

Nadia, Olenskyj, et al. (2021) reported distinct breakdown rates (measured as half-softening times, which were estimated using the Weibull model) of various solid starch-based foods in the proximal and distal stomach of growing pigs. The foods used were made of commonly consumed starch sources (durum wheat and long grain white rice), with varying physical structures as a result of food processing (intact grain, finely milled grain, couscous/agglomerated finely milled grain, and noodle/starch gel of finely milled grain). They found that the starch source, physical structure, and breakdown rate of the structure during gastric digestion impacted their gastric emptying rate. The different breakdown rates were thought to be influenced by distinct digesta pH between the stomach regions (proximal pH > distal pH). However, the simultaneous processes of gastric secretion, gastric emptying, and mechanical breakdown by gastric wall contractions *in vivo* limited the specific examination of the contribution of the proximal and distal gastric phases on food breakdown. Based on these *in vivo* observations, this study sought to investigate the roles of proximal and distal gastric digestion phases on the physicochemical properties of food particles and emptied particles for varying food structures studied by Nadia, Olenskyj, et al. (2021).

For the first time, the role of the proximal gastric digestion phase in solid starch-based foods, which has been commonly neglected in *in vitro* studies, was investigated in detail in this study. Understanding food breakdown during different phases of gastric digestion will be beneficial to improving food structuring strategies intended for controlled release of nutrients, especially through ingredient selection (e.g., starch source and intact/milled grain) and processing method. A static digestion approach was selected to isolate the roles of α-amylase during the proximal phase and gastric fluid during the distal phase of gastric digestion, while minimizing mechanical breakdown of the bolus. The experimental study was coupled with an empirical modelling approach to quantitatively compare the overall digestion kinetics between the foods studied and across different digestion treatments, as well as to provide quantitative comparisons with previous studies (such as the work of Drechsler and Bornhorst (2018) and Nadia, Olenskyj, et al. (2021)).

2. Materials and methods

2.1. Materials

Wheat couscous ('couscous'), wheat fettuccine ('pasta'), rice couscous, rice grain, rice noodle were used as described in Nadia, Olenskyj, et al. (2021). Couscous and rice couscous were sieved to obtain fractions with 1–2-mm diameter. Pasta and rice noodle were manually cut to 10–15 mm length prior to cooking, to maintain the size within a range comparable to what has been reported after mastication of similar products (Hoebler, Devaux, Karinthi, Belleville, & Barry, 2000; Ranawana, Henry, & Pratt, 2010). Foods were cooked following according to a standardized cooking procedure described by Nadia, Olenskyj, et al. (2021) to ensure the foods were completely cooked. Briefly, the couscous products were rehydrated with freshly boiled water (1:1.5 w/v) for 5 min; pasta and rice noodle were cooked (for 13 and 3 min, respectively) in boiled water (1:10 w/v) on a stovetop; rice grain was cooked (1:1.5 w/v rice:water ratio) using a commercial rice cooker (Kambrook, NZ) for 26 min. Preliminary experiments were completed to ensure that these cooking methods resulted in complete starch gelatinization of the cooked foods. Cooked foods were cooled to ~ 40 °C prior to analysis or *in vitro* digestion.

Simulated salivary fluid (SSF) and simulated gastric fluid (SGF) were formulated following INFOGEST standardized method (Brodkorb et al., 2019) with modifications in mucin addition and pH. All salts and pepsin were purchased from Sigma-Aldrich (MO, USA). Mucin type II (Sigma-Aldrich, MO, USA; MyBiosource, CA, USA) was added to the simulated digestive fluids at a concentration of 1 g/L SSF and 1.5 g/L SGF (Swackhamer, Zhang, Taha, & Bornhorst, 2019). SSF was prepared at pH 7 and was mixed with porcine pancreatic α-amylase (109 U/mg; 75 U/mL SSF; Megazyme, Ireland). SGF was prepared at pH 1.8 and was mixed with pepsin from porcine gastric mucosa (622 U/mg; 2000 U/mL SGF). No lipase was added because the foods had low fat content (Minekus et al., 2014). The SSF and SGF were re-adjusted to pH 7 and 1.8, respectively, after mixing with enzymes, and were warmed to 37 °C prior to digestion experiments.

2.2. Static in vitro digestion procedure

The digestion procedure was a shaking water bath digestion, of which the digestion condition and duration were designed based on the movement of food bolus from different locations of proximal stomach to the acidic distal stomach (Fig. 1A). It consisted of an oral phase, followed by two stages of gastric phase (Fig. 1B): proximal phase (prolonged incubation in SSF after the oral phase) and distal phase (sequential incubation in SGF). The extended incubation in SSF after the oral phase was referred to as the 'proximal phase', since such condition was found in the proximal stomach in studies using growing pigs (Bornhorst, Rutherfurd, et al., 2014; Nadia, Olenskyj, et al., 2021). For each food, experiments were conducted in batches; one experimental batch consisted of one proximal phase duration followed by immediate sampling (proximal digestion) or distal digestion (proximal–distal digestion). Each digestion was conducted in a container with a lid, where each container represented one replicate for one food and one proximal or proximal–distal digestioncondition. Triplicate digestions (i.e., three batches of experiments) were conducted for each food and digestion condition.

The oral phase was simulated by mixing 60 g cooked food with SSF (1:1 mL SSF/g dry matter of food) in a closed container (Brodkorb et al., 2019). The food-SSF mixture was incubated in a shaking water bath (37 °C, 35 rpm) for 30 s (Hoebler et al., 2000). The proximal phase was simulated by extending the oral phase incubation time for 2, 15, or 30 min, or without extension (0 min). There was a unique container for each proximal phase, such that the entire content of the container was removed at the end of each digestion condition. For proximal digestion not followed by the distal phase (proximal digestion), each sample

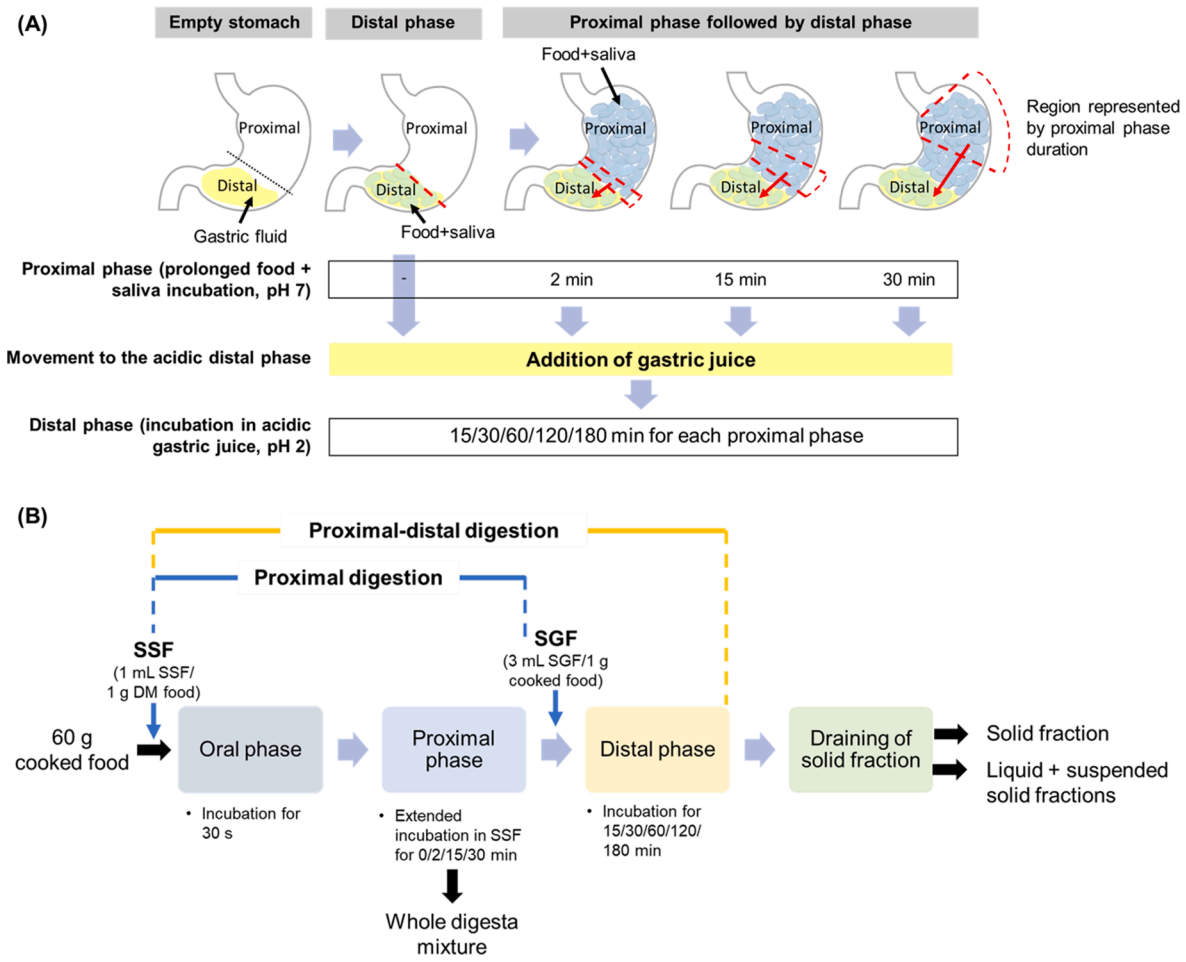

Fig. 1. Schematic diagram illustrating the rationale behind the experimental design. The filling of the proximal stomach results in different locations of food bolus in this region, thus different contact time with α-amylase, as this gastric content moves into the distal stomach region during the digestion process. Approximate intragastric regions of interest simulated by the different proximal durations are highlighted by red dashed lines. The red arrow in each proximal phase scenario indicates the movement of food bolus from the intragastric proximal region of interest to the distal phase (A). Block flow diagram of the different steps for proximal or proximal–distal digestion experiments, indicating the times utilized in each phase of digestion, and the samples utilized for further analysis (B).

container was removed from the water bath after the proximal phase (0/2/15/30 min proximal digestion). The entire digestion mixture from the proximal digestion was mixed with 0.4 mL of 6 M NaOH to reach uniform pH (pH ~10) to terminate enzymatic reactions without changing the physical properties. The proximal phase samples were treated as a whole digesta mixture in the subsequent analyses, as the free liquid was not easily removable in most samples.

For proximal followed by distal phase digestion (proximal–distal digestion), after a selected proximal phase, 180 mL SGF was added (3 mL SGF/g cooked food) to the food-SSF mixture and gently mixed, then incubated in a shaking water bath (37 °C, 35 rpm) for an additional 15, 30, 60, 120, or 180 min to simulate the distal phase. After 5 and 10 min of SGF addition, the pH of the mixture was adjusted to pH 2 ± 0.1 with 6 M HCl. When necessary, the pH was readjusted 60 min after SGF addition. The volume of HCl used for pH adjustment was between 0.14 and 0.30% of the volume of SGF added. The sample container was removed from the water bath after a selected distal phase time point (15/30/60/120/180 min), then the remaining solid (solid fraction) was drained from the liquid-suspended solid mixture using a flexible mesh (1 × 2 mm aperture), based on the typical size of particles (1–2 mm in diameter) that would undergo gastric sieving (Meyer, Elashoff, Porter-Fink, Dressman, & Amidon, 1988). The solid fraction was weighed, then mixed with 0.8 mL of 6 M NaOH to reach uniform pH (pH ~10). On the same day, the solid fraction was analyzed for texture, moisture content, and particle size; the liquid-suspended solid mixture was analyzed for total soluble solids and particle size. Subsamples of liquid-suspended solid mixture (0.95 mL aliquot mixed with 0.05 mL of 2 M NaOH) were frozen at −20 °C until analysis.

2.3. Cooked food, solid digesta and whole digesta characterization

2.3.1. Moisture content

Moisture content was determined gravimetrically in duplicate at 105 °C in a convection oven until constant weight (~16–20 h) (Nadia, Olenskyj, et al., 2021).

2.3.1.1. Texture analysis. Sample was added to a 42-mm inner diameter back-extrusion cell to ~15 mm height, and the surface was gently flattened. The sample was compressed at 1 mm/s to 50% strain using a 37-mm diameter plunger attached to a texture analyzer (TA.XT HD, Stable Micro Systems, Surrey, UK). Hardness was calculated as the peak force (N) during compression. For undigested food, samples were mixed with water at 1:1 (mL water:g dry matter of food) ratio prior to measurement; this was done to minimize the interference of void spaces on the textural measurement (Drechsler & Bornhorst, 2018). Analyses were conducted on at least two aliquots of each sample.

2.3.1.2. Particle size. The particle size of the solid fraction was determined using an image analysis procedure (Nadia, Olenskyj, et al., 2021) without staining using KI solution. Duplicate samples were analysed

after the proximal phase, and after 30 and 180 min distal phase for each proximal phase duration. Two images were taken per sample from each replicate, and results from image processing from the two images were averaged to represent that particular sample. After image processing in MATLAB R2018a as described by Nadia, Olenskyj, et al. (2021) to obtain the area of all particles present in each image, particles $<0.05\ mm^2$ were not considered to minimize noise in results.

2.4. Liquid and suspended solid characterization

2.4.1. Total soluble solids

Total soluble solids (^{o}Brix) in the liquid-suspended solid mixture were quantified using a digital refractometer (PAL-1 Pocket Refractometer, Atago, Japan). Each sample was measured three times. The ^{o}Brix of SGF and SSF were considered as controls.

2.4.1.1. Particle size. Particle size of the liquid-suspended solid mixture (two aliquots per sample) was measured using Mastersizer-2000 (Malvern Instruments Ltd., Worcestershire, UK) with a refractive index of 1.530 for starch-based samples (Angelidis, Protonotariou, Mandala, & Rosell, 2016).

2.5. Hydrolyzed starch content

Frozen samples were thawed and centrifuged (6,800 × *g*, 10 min) to separate the suspended solids. The liquid fraction was used directly for analysis. The suspended solid fraction (0.1 g) was mixed with 1.5 mL water, incubated 1 h at room temperature, centrifuged (6,800 × *g*, 10 min), and the supernatant (0.1–0.4 mL) was analyzed.

Maltose content was quantified using the dinitrosalicylic acid method adapted to 96-well microplates (Tagle-Freire et al., 2022). The absorbance of triplicate aliquots of each sample was read at 540 nm using a microplate reader (SPECTROstar Nano, BMG Labtech, Germany).

Starch content of cooked food was determined in freeze-dried samples using Megazyme Total Starch Kit (Megazyme, Wicklow, Ireland), following the procedure for samples not containing free sugars or resistant starch. Hydrolyzed starch content in sample was expressed as g maltose/g starch in its respective cooked food.

2.6. Data and statistical analysis

2.6.1. Solid retention calculation

The Mitscherlich equation on the "law of diminishing increments" was selected (Harmsen, 2000) to empirically describe the asymptotic behavior of the solid retention data during the proximal–distal digestions:

$$\frac{M_t}{M_0} = A - (A - A_0)e^{-k_m \cdot t} \quad (1)$$

where M_t: dry or wet mass (g) of the digesta at distal time t; M_0: initial dry mass (g) of the cooked food for each digestion; A: the asymptote value of the curve (unitless); A_0: theoretical initial mass retention without proximal phase (equals to one; unitless); k_m: a coefficient describing the rate of mass retention change (min^{-1}). Model fitting (nonlinear least squares method) was conducted in MATLAB R2018a (The MathWorks Inc., Natick, MA, USA).

2.6.2. Softening kinetics of solid fraction and whole digesta mixture

Softening kinetics were determined by fitting texture data to the Weibull model (Drechsler & Bornhorst, 2018):

$$\frac{H_t}{H_0} = e^{-(k_h \cdot t)^{\beta_h}} \quad (2)$$

where H_t: the hardness of the digesta (N) at time t (min); H_0: the initial hardness of the food (N) measured with water addition; k_h: the scale parameter of the softening curve (min^{-1}); β_h: the shape factor of the softening curve (unitless).

Model fitting (nonlinear least squares method) was conducted in MATLAB R2018a. Fitting of proximal digestion data was conducted on the data points from all three replicates together (Figure S1) because experiments for different proximal times within each replicate were conducted on different days. For each proximal phase, fitting of proximal–distal digestion data was conducted on each replicate (Figure S2). The half-softening time ($t_{1/2,softening}$) for proximal digestion was estimated by re-parameterizing k_h in Eqn. (2) as $k_h = \left[(\ln 2)^{1/\beta_h}\right] \Big/ t_{1/2,softening}$, which was derived from Eqn. (2) by defining $H_t/H_0 = 0.5$ and $t = t_{1/2,softening}$, while the $t_{1/2,softening}$ for proximal–distal digestion was calculated using the obtained k_h and β_h parameters for each replicate.

2.6.3. Particle size parameters of cooked food and solid fraction

Particle size data from image analysis were fit to the Rosin-Rammler model in MATLAB R2018a using the nonlinear least squares method (Hutchings et al., 2011):

$$Q = 1 - e^{-\left(x/x_{50}\right)^b} \cdot \ln(2) \quad (3)$$

where Q: the cumulative particle area (% of total area); x: n^{th} area measurement (mm^2); x_{50}: the area of a theoretical sieve aperture through which 50% of the particle area can pass (mm^2); b: the broadness of the distribution (dimensionless).

The x_{10} and x_{90} (the area of a theoretical sieve aperture through which 10% and 90% of the particle area can pass, respectively) were calculated using Eqn. (3). The total particle area and the number of particles in each sample were utilized to calculate the particle area per gram digesta, number of particles per gram dry matter, and average area per particle.

2.6.4. Statistical analysis

Statistical analysis was conducted in SAS®Studio 3.8 (SAS Institute, Cary, NC, USA). The normality and heteroscedasticity of the properties data of undigested foods were assessed with Shapiro-Wilk's test and Levene's test, respectively. The moisture content, hardness, particle size, starch content, hydrolyzed starch content of undigested foods were analyzed with one-way ANOVA. The particle size parameters of undigested foods were analyzed with the Kruskal-Wallis test.

For digesta properties, a mixed model ANOVA (PROC GLIMMIX) was employed. The experimental unit was the batch of experiments. The effect of food type, proximal phase, and their interaction was analyzed on particle size parameters and hardness data from proximal digestion, as well as model parameters of solid retention (Eqn. (1)) and softening kinetics (Eqn. (2)) from proximal-distal digestion. The effect of food type, proximal and distal phase, and their interaction effects were analyzed on the characteristics of solid (moisture content, solid retention, hardness, particle size parameters) and liquid-suspended solid fractions ($^{\circ}$Brix, particle size parameters, and hydrolyzed starch content) of digesta from proximal-distal digestion. Logarithmic transformation was applied to all particle size parameters (both on the solid and liquid-suspended solid fractions), $t_{1/2,softening}$, and k_h to achieve normality of residuals.

Preliminary statistical analyses were conducted on all data sets to remove outliers (internally studentized residuals outside (-3, 3)). When main effects were significant, the Tukey-Kramer procedure was used to identify differences between individual means at a significance level of $p < 0.05$. All values are presented as mean ± standard deviation (SD).

3. Results

3.1. Characteristics of the selected food products

The average area per particle, x_{10}, x_{50}, and x_{90} of the undigested,

cooked foods were significantly different between the five foods ($p < 0.01$; Table 1). Overall, the general trend in these particle size parameters was: agglomerated products (couscous, rice couscous) < rice grain < noodles (pasta, rice noodle). The hardness (measured with lubrication) followed the order: rice grain (112.59 ± 8.72 N) > agglomerated products (66.39 ± 11.87 N) > noodle products (51.46 ± 9.67 N).

3.2. Whole digesta mixture properties after proximal digestion

Normalized hardness (H_t/H_0) during proximal digestion was significantly influenced by food type and proximal phase time ($p < 0.0001$; Table S1). The $t_{1/2,softening}$ of the foods during proximal digestion was significantly influenced by food type ($p < 0.0001$; Fig. 2A). Among the foods, agglomerated products had the shortest $t_{1/2,softening}$ (<1 min), followed by rice noodle (123.5 min), rice grain (355.9 min), and pasta (541.8 min).

Across the foods, only rice grain exhibited a significant decrease in particle size parameters x_{10} and x_{50} between 0 and 30 min proximal phase (Table S4; $p < 0.05$). Compared to the undigested food, an increasing proportion of particles ≤4 mm^2 with a longer proximal phase was observed in rice grain and noodles (from 1.42% to 3.52% at 0 and 30 min proximal phase, averaged across rice grain and both noodles, respectively). Similarly, an increasing proportion of particles ≤4 mm^2 was observed in agglomerated products with longer proximal phase (from 37.88% to 44.02% at 0 and 30 min proximal phase, respectively, averaged across agglomerated products).

3.3. Properties of solid digesta fraction after proximal–distal digestion

Both wet and dry mass retention (W_t/W_0 and DM_t/DM_0, respectively) were influenced by all main effects and food × distal interaction ($p < 0.0001$; Table S1). The W_t/W_0 was measured to provide information on the simultaneous effect of SGF uptake into the food particles and leaching of solids that occurred during digestion, while the DM_t/DM_0 was measured to investigate true solid retention of the food particles as impacted by leaching of solids due to biochemical digestion and/or acid hydrolysis during digestion (Kong & Singh, 2009; Nadia, Olenskyj, et al., 2021). The DM_t/DM_0 of agglomerated products and pasta generally decreased asymptotically with longer distal phase (Fig. 3), while no significant change in DM_t/DM_0 was observed in rice noodle and rice grain across distal phase times ($p \geq 0.4984$).

The W_t/W_0 and DM_t/DM_0 during proximal–distal digestion fit well to the Mitscherlich equation (Table 2; Figure S8), with average $R^2 > 0.8$. Asymptote values obtained using Mitscherlich equation (Eqn. (1)) provided a quantitative description in the overall solid retention profile due to different foods and proximal phase durations. The asymptotes of W_t/W_0 and DM_t/DM_0 (A in Eqn. (1)) were significantly affected by food type and proximal phase ($p < 0.0001$; Table S1). For all foods, the asymptotes of both W_t/W_0 and DM_t/DM_0 decreased significantly with longer proximal phase, especially between 0 or 15 min proximal phase ($p < 0.05$; Table 2). Compared to rice grain and noodle products, agglomerated products underwent a larger reduction in the asymptotes of W_t/W_0 and DM_t/DM_0 due to the proximal phase. For instance, after 0 or 15 min proximal phase, the asymptotes of the DM_t/DM_0 during the proximal–distal digestion of agglomerated products were 0.78 ± 0.10 and 0.62 ± 0.08, respectively (averaged across agglomerated products). Meanwhile, for the three other foods and after 0 or 15 min proximal phase, the asymptotes of the DM_t/DM_0 were 0.95 ± 0.04 and 0.83 ± 0.06, respectively (averaged across non-agglomerated products).

All main effects and their interactions, except the proximal × distal interaction significantly ($p < 0.05$; Table S1) impacted normalized hardness (H_t/H_0) during proximal–distal digestion (Fig. 4). Fitting the H_t/H_0 data to the Weibull model (Eqn. (2)) enabled quantitative comparison of the softening behavior between foods and proximal phase durations, through the calculation of $t_{1/2,softening}$ using the obtained k_h and β_h parameters. The $t_{1/2,softening}$ of the solid digesta fraction during the distal phase was affected by food type ($p < 0.001$) and proximal phase ($p < 0.05$; Table S1). The food × proximal interaction was not significant to the $t_{1/2,softening}$, such that no notable changes in $t_{1/2,softening}$ were observed for any food with longer proximal phase time ($p > 0.05$; Table 2). At 0 min proximal phase the $t_{1/2,softening}$ of agglomerated products was lower ($p < 0.05$) than that of rice grain and noodle products (17.1 ± 16.4 vs. 308.6 ± 170.5 min, averaged between agglomerated products and the three other foods, respectively).

Moisture change in the solid fraction relative to the undigested food was calculated to compare the moisture uptake during gastric digestion (Fig. 4). Moisture change was affected by all main effects, and the food × proximal and food × distal interactions ($p < 0.01$; Table S1). All foods had increasing moisture content with longer distal phase. At any distal phase, moisture change followed the trend: agglomerated products > rice grain > noodle products. For example, moisture change after 15 min distal phase was 1.84 ± 0.21 vs. 0.99 ± 0.13 and 0.76 ± 0.21 g H_2O/g DM for agglomerated products vs. rice grain and noodle products, respectively (averaged across proximal phase).

Food type was significant ($p < 0.0001$) to all particle size parameters of the solid digesta fraction. The food × distal interaction was significant ($p < 0.01$) to all parameters except particle area/gram. The food × proximal interaction ($p < 0.05$; Table S1) only impacted x_{10}, x_{50}, and average area/gram. The food × proximal × distal interaction was not significant to any particle size parameter ($p > 0.05$).

Rice grain underwent a significant decrease in the x_{50} and x_{90} with longer proximal phase or longer distal phase ($p < 0.05$; Table 3 and S8). Between 30 and 180 min distal phase in rice grain and noodle products, particles/g DM increased, while the average area/particle decreased ($p < 0.05$; when averaged across proximal phase). Visualization of the particle area distribution of each food × proximal × distal combination (Fig. 2B-F and S3-S7; Table S5) provided additional information on

Table 1
Physical properties and chemical content of the selected undigested, cooked foods. Values are shown as mean ± SD (n = 6 for each data point). Significantly different values between foods within the same measured parameter are indicated with abcd superscript ($p < 0.05$).

Parameter	Couscous	Rice couscous	Pasta	Rice noodle	Rice grain
x_{10} (mm^2)	0.77 ± 0.42^c	0.20 ± 0.10^d	119.77 ± 27.35^a	89.67 ± 26.51^a	10.68 ± 2.12^b
x_{50} (mm^2)	5.41 ± 1.92^c	4.03 ± 1.99^c	228.8 ± 50.64^a	195.94 ± 15.44^a	35.5 ± 6.91^b
x_{90} (mm^2)	11.22 ± 3.48^c	12.43 ± 6.09^c	296.54 ± 77.97^a	266.83 ± 20.11^a	56.08 ± 13.28^b
b (dimensionless)	1.64 ± 0.17^c	1.07 ± 0.06^d	5.70 ± 1.91^a	4.43 ± 1.45^{ab}	2.77 ± 0.41^b
Specific surface area (mm^2/gram)	1886.0 ± 507.5^a	2419.9 ± 294.0^a	788.9 ± 141.8^c	1274.7 ± 48.8^b	912.3 ± 177.1^c
Average area (mm^2)/particle	3.17 ± 1.18^c	1.55 ± 0.57^c	69.86 ± 19.87^a	62.89 ± 39.39^a	10.4 ± 2.18^b
Particles/g DM	1728 ± 296^b	4432 ± 1170^a	35 ± 12^d	95 ± 79^d	230 ± 23^c
Moisture content (g H_2O/g DM)	1.79 ± 0.06^a	1.60 ± 0.08^b	1.87 ± 0.07^a	1.78 ± 0.11^a	1.61 ± 0.09^b
Initial hardness (N)[†]	74.21 ± 9.73^b	58.58 ± 8.29^{bc}	56.07 ± 9.56^c	46.86 ± 7.97^c	112.59 ± 8.72^a
Starch content (g/100 g DM)	67.16 ± 2.30^b	82.36 ± 1.76^a	71.43 ± 4.86^b	81.9 ± 3.55^a	82.38 ± 2.87^a
Hydrolyzed starch content(g maltose/g starch)[*]	0.020 ± 0.003^a	0.004 ± 0.001^b	0.018 ± 0.004^a	0.004 ± 0.002^b	0.003 ± 0.001^b

[†] Measured with water addition (1 mL water:1 g DM food).
[*] Maltose content was measured in homogenized, cooked food as described for the suspended solid digesta fraction.

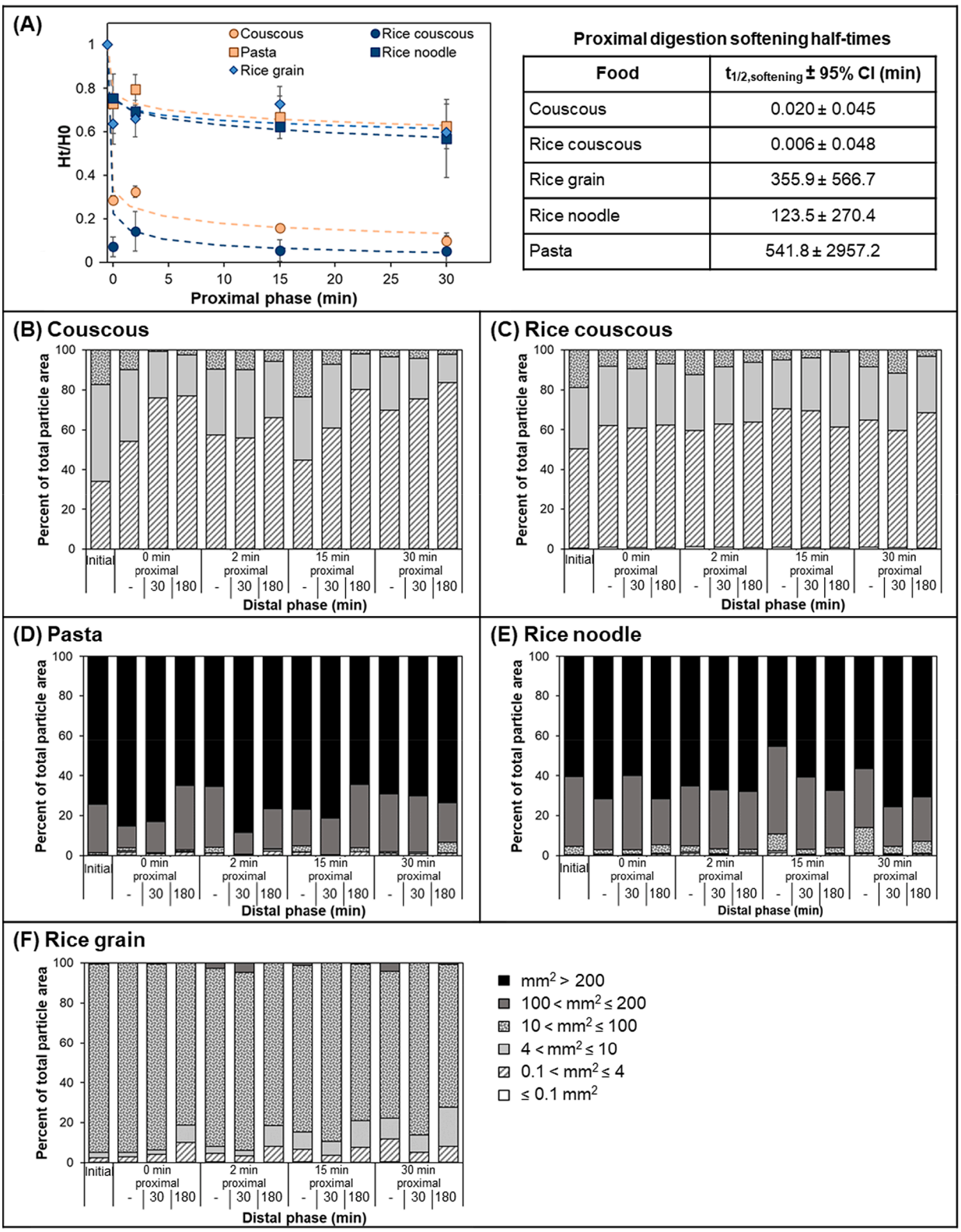

Fig. 2. Textural changes of the foods after being subjected to various proximal phase durations in the proximal digestion. The hardness at each time (H_t, Table S2) was normalized by the hardness of undigested foods (H_0) with lubrication. Values are shown as mean ± SD (n = 3 for each data point). The dashed lines are the Weibull model (Eqn. (2)) fit with average softening kinetics parameters (Table S3). The $t_{1/2,softening}$ values and their 95% confidence interval (CI) were estimated through the re-parameterization of Eqn. (2) (A). Bar graphs showing the particle area distribution of couscous (B), rice couscous (C), pasta (D), rice noodle (E), and rice grain (F) before digestion (Initial), whole digesta mixture after different proximal phase durations (shown as "-" in the distal phase), and digesta solid fraction after selected proximal × distal phase in proximal–distal digestion. Bins constituting each bar graph were pooled data from three replicates (see Figure S3-S7 for the histogram constituting each bar graph). The exact value for each area bin can be found in Table S5.

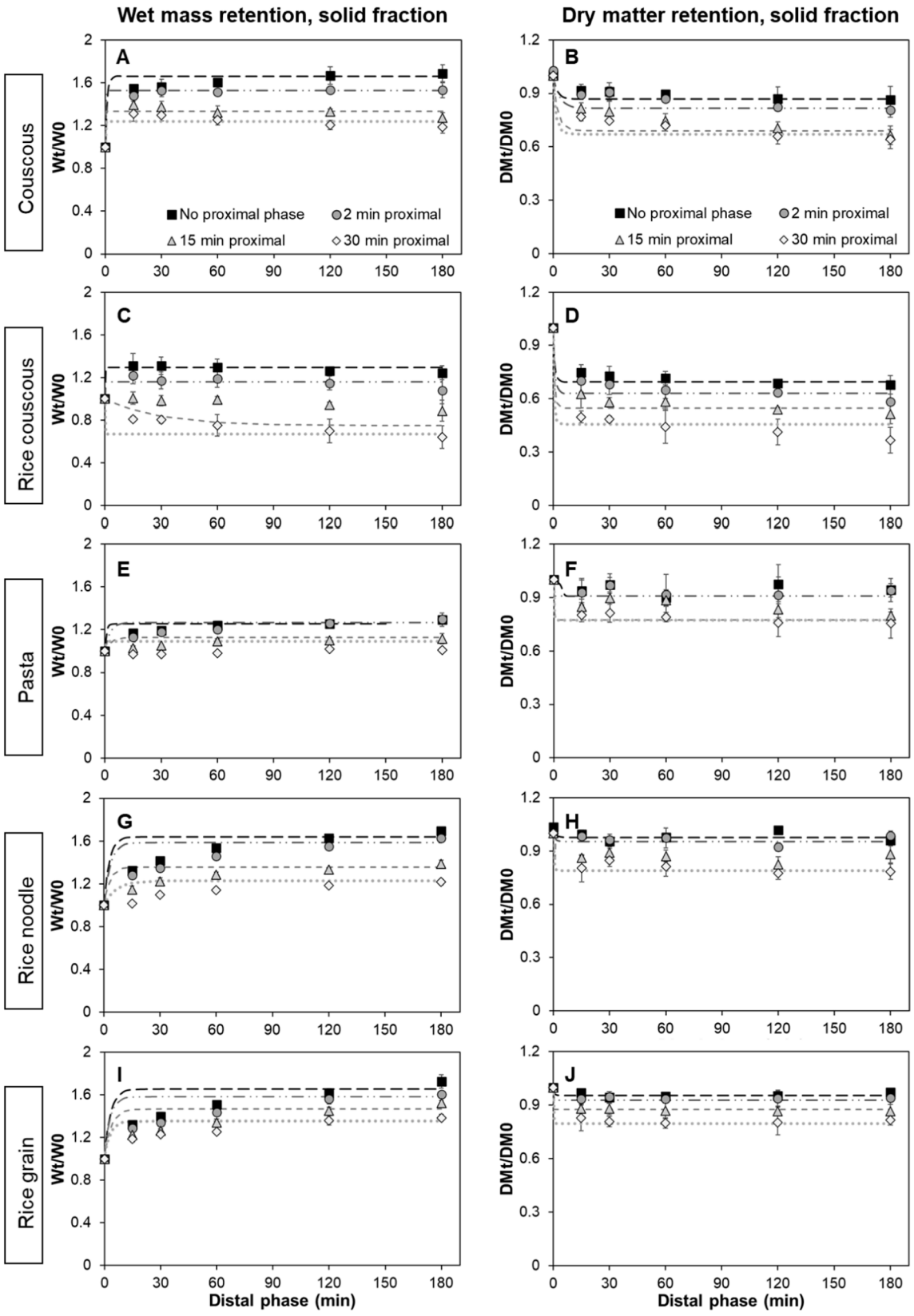

Fig. 3. Wet mass retention (W_t/W_0; dimensionless) and dry matter retention (DM_t/DM_0; dimensionless) profiles of the solid fraction of digesta during the distal phase after 0 min (■), 2 min (●), 15 min (△), or 30 min (◇) proximal phase. Figures within the same row correspond to one type of food: couscous (A-B), rice couscous (C-D), pasta (E-F), rice noodle (G-H), and rice grain (I-J). All values were normalized against the wet mass or dry matter of the cooked (undigested) food used in each sample. Values are shown as mean ± SD (n = 3 for each data point, except rice couscous 15 min proximal-180 min distal, n = 2 due to outlier removal). Lines indicate Mitscherlich equation (Eqn. (1)) fit with average parameters (Table 2) at 0 min (□ □ □), 2 min (—·—), 15 min (- - -), or 30 min (···) proximal phase. See Figure S8 for model fit to individual datasets.

Table 2
Mitscherlich equation (Eqn. (1)) parameters of mass retention profile of digesta solid fraction and softening kinetic parameters of digesta solid fraction for proximal–distal digestion, at various proximal phase durations. k_m: a coefficient describing the rate of mass retention change, A: asymptote values of the mass retention curve; k_h: the scale parameter in the softening kinetics curve, β_h: the shape factor in the softening kinetics curve; $t_{1/2,softening}$: softening half-time. The goodness of fit of the model to the data points is indicated by $R^2$and RMSE (root-mean-square-error). Values are shown as mean ± SD (n = 3 for all parameters for each food × proximal phase duration and parameter, except values indicated with asterisk (*), n = 2 due to outlier removal). For a single parameter, significantly different values between proximal phase for one type of food are indicated with abcd superscript. Significantly different values between food types within the same proximal phase are indicated with zyxw superscript ($p < 0.05$).

Food	Proximal phase (min)	Wet mass retention				Dry mass retention				Softening kinetics				
		k_m (×10 min^{-1})	A (unitless)	R^2	RMSE (×10)	k_m (×10 min^{-1})	A (unitless)	R^2	RMSE (×10)	k_h (×100 min^{-1})	β_h (unitless)	R^2	RMSE (×10)	$t_{1/2,softening}$ (min)
Couscous	0	1.13 ± 0.13^{b,zy}	1.66 ± 0.07^{a,z}	0.97 ± 0.01	0.50 ± 0.10	0.47 ± 0.33	0.87 ± 0.06^{a,y}	0.85 ± 0.13	0.22 ± 0.06	4.54 ± 0.33^{z}	0.64 ± 0.04^{zy}	0.99 ± 0.00	0.32 ± 0.07	12.5 ± 1.33^{y}
	2	4.95 ± 6.23^{b,z}	1.53 ± 0.03^{b,z}	0.99 ± 0.00	0.27 ± 0.06	0.30 ± 0.07	0.82 ± 0.02^{a,y}	0.87 ± 0.06	0.27 ± 0.08	3.77 ± 1.21^{z}	0.57 ± 0.16	1.00 ± 0.00	0.23 ± 0.14	15.5 ± 8.83^{y}
	15	18.95 ± 4.29^{a,z}	1.33 ± 0.04^{c,zy}	0.92 ± 0.05	0.44 ± 0.16	0.41 ± 0.16	0.69 ± 0.03^{b,x}	0.96 ± 0.02	0.27 ± 0.08	3.58 ± 1.98^{z}	0.61 ± 0.07	1.00 ± 0.00	0.16 ± 0.04	18.4 ± 8.21
	30	11.93 ± 1.12^{ab,z}	1.24 ± 0.05^{c,z}	0.79 ± 0.10	0.58 ± 0.17	0.68 ± 0.19	0.67 ± 0.05^{b,y}	0.95 ± 0.02	0.33 ± 0.09	7.40 ± 7.45^{z}	0.58 ± 0.27^{zy}	0.99 ± 0.01	0.31 ± 0.30	13.5 ± 10.0^{y}
Rice couscous	0	11.40 ± 9.55^{ab,z}	1.29 ± 0.06^{a,y}	0.92 ± 0.10	0.36 ± 0.39	1.16 ± 0.40	0.70 ± 0.03^{a,x}	0.97 ± 0.03	0.22 ± 0.11	*3.51 ± 4.38^{zy}	0.16 ± 0.08^{y}	0.99 ± 0.01	0.25 ± 0.21	*24.0 ± 30.3^{y}
	2	10.49 ± 0.53^{a,z}	1.16 ± 0.07^{b,y}	0.54 ± 0.30	0.65 ± 0.29	1.04 ± 0.54	0.63 ± 0.02^{b,x}	0.98 ± 0.01	0.24 ± 0.09	1.70 ± 0.81^{z}	0.40 ± 0.23	0.99 ± 0.01	0.30 ± 0.13	27.5 ± 24.1^{y}
	15	0.03 ± 0.03^{c,x}	0.75 ± 0.26^{c,w}	0.52 ± 0.31	0.40 ± 0.12	1.30 ± 0.54	0.55 ± 0.01^{c,w}	0.98 ± 0.01	0.26 ± 0.09	*0.09 ± 0.10^{zy}	0.18 ± 0.08	0.91 ± 0.08	0.64 ± 0.26	151.1 ± 145.2
	30	8.49 ± 14.29^{b,y}	0.67 ± 0.12^{d,y}	0.91 ± 0.12	0.36 ± 0.27	1.73 ± 0.13	0.46 ± 0.01^{d,x}	0.93 ± 0.07	0.59 ± 0.42	0.51 ± 0.27^{zy}	0.87 ± 0.33^{zy}	0.96 ± 0.02	0.49 ± 0.08	158.7 ± 97.7^{zy}
Pasta	0	0.52 ± 0.16^{a,y}	1.26 ± 0.04^{a,y}	0.98 ± 0.00	0.16 ± 0.04	0.27 ± 0.23	*0.91 ± 0.06^{a,zy}	0.50 ± 0.42	0.36 ± 0.26	0.19 ± 0.10^{zy}	0.63 ± 0.35^{b,zy}	0.86 ± 0.1	0.73 ± 0.38	280.4 ± 39.0^{z}
	2	0.38 ± 0.18^{a,y}	1.27 ± 0.04^{a,y}	0.97 ± 0.01	0.22 ± 0.06	10.29 ± 17.06	0.91 ± 0.10^{a,zy}	0.59 ± 0.25	0.30 ± 0.06	0.13 ± 0.11^{y}	0.78 ± 0.41^{b}	0.63 ± 0.21	0.86 ± 0.41	1276.5 ± 1536.4^{z}
	15	0.32 ± 0.29^{a,y}	1.13 ± 0.05^{b,x}	0.97 ± 0.03	0.09 ± 0.06	3.75 ± 6.24	0.77 ± 0.08^{b,yx}	0.81 ± 0.06	0.37 ± 0.07	0.17 ± 0.13^{zy}	0.75 ± 0.44^{b}	0.78 ± 0.08	0.90 ± 0.32	857.8 ± 1043.1
	30	2.33 ± 4.02^{b,x}	1.09 ± 0.11^{b,x}	0.19 ± 0.20	0.23 ± 0.12	4.12 ± 5.33	0.77 ± 0.06^{b,z}	0.91 ± 0.01	0.31 ± 0.09	0.21 ± 0.17^{y}	*1.83 ± 0.25^{a,z}	0.70 ± 0.13	0.99 ± 0.16	1719.1 ± 2514.1^{z}
Rice noodle	0	0.37 ± 0.05^{y}	1.64 ± 0.03^{a,z}	0.98 ± 0.00	0.36 ± 0.01	0.50 ± 0.52	0.97 ± 0.03^{a,z}	0.33 ± 0.33	0.24 ± 0.13	0.09 ± 0.08^{y}	0.41 ± 0.21^{zy}	0.76 ± 0.25	0.81 ± 0.57	491.4 ± 165.7^{z}
	2	0.31 ± 0.03^{y}	1.58 ± 0.03^{a,z}	0.96 ± 0.01	0.50 ± 0.04	1.05 ± 1.31	0.95 ± 0.003^{a,z}	0.62 ± 0.25	0.23 ± 0.12	0.12 ± 0.09^{y}	0.47 ± 0.15	0.60 ± 0.45	0.89 ± 0.38	1115.5 ± 1430.5^{z}
	15	0.33 ± 0.14^{y}	1.36 ± 0.04^{b,zy}	0.99 ± 0.02	0.15 ± 0.13	3.37 ± 5.13	0.85 ± 0.03^{b,zy}	0.80 ± 0.07	0.32 ± 0.07	0.04 ± 0.05^{y}	0.44 ± 0.04	0.83 ± 0.21	0.43 ± 0.30	2910.9 ± 2116.4
	30	0.16 ± 0.02^{y}	1.23 ± 0.03^{c,z}	0.99 ± 0.01	0.11 ± 0.07	3.38 ± 5.18	0.79 ± 0.03^{c,z}	0.93 ± 0.06	0.25 ± 0.13	0.12 ± 0.18^{y}	0.58 ± 0.43^{y}	0.63 ± 0.28	0.70 ± 0.29	1329.3 ± 978.0^{z}
Rice grain	0	0.31 ± 0.03^{y}	1.66 ± 0.07^{a,z}	0.96 ± 0.02	0.53 ± 0.18	1.43 ± 1.09	0.95 ± 0.01^{a,zy}	0.69 ± 0.24	0.15 ± 0.06	0.48 ± 0.04^{zy}	1.27 ± 0.47^{z}	0.92 ± 0.12	0.63 ± 0.61	153.9 ± 10.3^{z}
	2	0.34 ± 0.06^{y}	1.58 ± 0.03^{ab,z}	0.97 ± 0.02	0.40 ± 0.09	3.03 ± 4.18	0.93 ± 0.02^{ab,z}	0.71 ± 0.14	0.19 ± 0.08	0.26 ± 0.21^{zy}	0.71 ± 0.38	0.86 ± 0.13	0.66 ± 0.12	572.8 ± 691.3^{z}
	15	0.30 ± 0.03^{y}	1.47 ± 0.02^{b,z}	0.94 ± 0.03	0.47 ± 0.09	9.92 ± 14.41	0.88 ± 0.02^{b,z}	0.89 ± 0.08	0.19 ± 0.11	0.18 ± 0.05^{zy}	0.67 ± 0.25	0.76 ± 0.31	0.76 ± 0.62	329.0 ± 68.4
	30	0.36 ± 0.01^{y}	1.35 ± 0.01^{c,zy}	0.93 ± 0.04	0.39 ± 0.13	3.82 ± 5.58	0.80 ± 0.01^{c,z}	0.91 ± 0.02	0.28 ± 0.03	0.13 ± 0.19^{y}	0.56 ± 0.35^{y}	0.80 ± 0.12	0.59 ± 0.14	1322.1 ± 1310.3^{z}

Note: values with standard deviation noted as 0.00 have very small standard deviation (SD < 0.005), but was rounded down to 0.00.

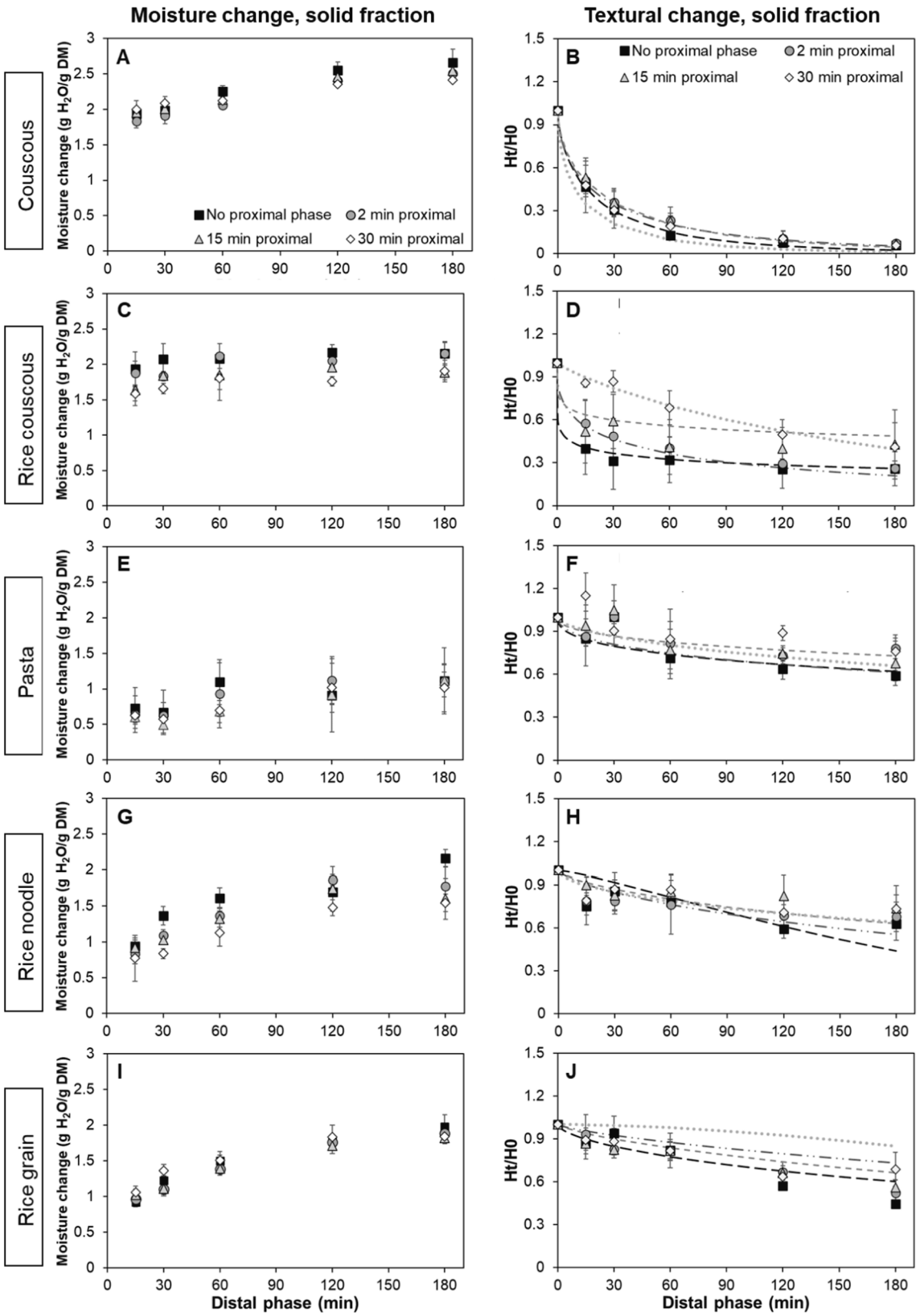

Fig. 4. Moisture change and normalized hardness (H_t/H_0) profiles of the solid fraction of digesta during the distal phase after 0 min (■), 2 min (●), 15 min (▲), or 30 min (◇) proximal phase. Figures within the same row correspond to one type of food: couscous (A-B), rice couscous (C-D), pasta (E-F), rice noodle (G-H), and rice grain (I-J). For each food, moisture change at each distal phase duration was calculated as the relative change of the moisture content of digesta (Table S7) from the moisture content of undigested food (Table 1). Hardness value (H_t, Table S6) was normalized against the hardness of undigested food (H_0); normalized hardness at 0 min distal phase was set to 1 for all proximal phase durations. Values are shown as mean ± SD (n = 3 for each data point). Lines in the H_t/H_0 graphs indicate the Weibull model fit (Eqn. (2)) with average parameters (Table 2) at 0 min (□ □ □), 2 min (—·—), 15 min (- - -), or 30 min (···) proximal phase. See Figure S2 for model fit to individual datasets.

particle size changes during proximal–distal digestion. Couscous and rice couscous digesta had less particles between 10 and 100 mm^2 at 30 or 180 min distal phase compared to their undigested condition (6.89, 3.69, and 18.04%, respectively; averaged across the agglomerated products and proximal phase). Particles > 100 mm^2 in pasta and rice noodle digesta slightly decreased between 30 and 180 min distal phase (97.69 and 95.42%, respectively; averaged across the noodles and proximal phase). The proportion of particles between 10 and 100 mm^2 in rice grain digesta decreased between 30 or 180 min distal phase (89.45 and 78.24%, respectively; averaged across proximal phase).

3.4. Properties of liquid and suspended solid digesta fractions after the proximal and distal phase

All main effects, food × proximal, and food × distal interactions significantly influenced D[4,3], D[3,2], d_{10}, d_{50}, d_{90}, °Brix, and hydrolyzed starch content of the liquid and suspended solid digesta fractions ($p < 0.05$; Table S1). Longer distal phase generally increased the D[4,3] and D[3,2] in wheat-based foods, especially at proximal phase ≤ 15 min for couscous and proximal phase ≤ 2 min for pasta (Table 4). Longer proximal phase duration generally decreased the D[4,3] in all rice-based foods and D[3,2] in pasta, rice couscous, and rice grain (Table 4).

The particle size distribution profile of the suspended solid fraction was multimodal in most samples except rice noodle (Fig. 5), thus d_{10}, d_{50}, and d_{90} (Table S9) were not assessed further. For wheat-based foods, the peak which initially appeared between 20 and 40 μm after 15 min distal phase shifted to a larger size with longer distal phase. For all rice-based foods, with longer proximal phase, the maximum %volume of the peak occurring between 5 and 15 μm increased and the peak between 100 and 1000 μm disappeared (Fig. 5).

°Brix, which represented the amount of soluble solids in the liquid digesta fraction, increased with longer proximal and distal phase for all foods (Fig. 6; $p < 0.05$). The increase was larger with longer proximal phase rather than the distal phase. For example, when the proximal phase was extended to 30 min, the °Brix values for rice grain were 1.61 ± 0.25 and 2.28 ± 0.18 after 15 and 180 min distal phase, respectively. The °Brix was always the highest in agglomerated products compared to the three other foods. For instance, the °Brix of agglomerated products, rice grain, and noodle products were 1.07 ± 0.20, 0.25 ± 0.14, and 0.30 ± 0.11, respectively, after 15 min distal phase preceded by no proximal phase (averaged across products within the same category).

Hydrolyzed starch content increased with longer proximal phase for all foods, regardless of the distal phase duration (Fig. 6; $p < 0.05$). At any proximal and distal phase, agglomerated products had higher hydrolyzed starch compared to the three other foods. For example, after 30 min proximal phase followed by 180 min distal phase (maximum digestion duration), the hydrolyzed starch content in agglomerated products and non-agglomerated products was 0.54 ± 0.24 and 0.39 ± 0.13 g maltose/g starch, respectively. In agglomerated products, the hydrolyzed starch content after 180 min distal phase was significantly higher than 15 min distal phase, when preceded by 15 or 30 min of proximal phase ($p \leq 0.0025$). For instance, 30 min of proximal phase digestion in rice couscous followed by 15 or 180 min of distal phase digestion increased starch hydrolysis from 0.51 ± 0.03 to 0.74 ± 0.14 g maltose/g starch, respectively ($p < 0.0001$).

4. Discussion

4.1. Changes to whole digesta mixture during the proximal phase

During proximal digestion, a longer proximal phase duration reduced the hardness of the whole digesta, as a result of longer contact with α-amylase and SSF uptake in the absence of gastric fluid. Softening occurred at different rates for the different foods. Based on their $t_{1/2,softening}$ during the proximal phase, couscous and rice couscous (agglomerated products, $t_{1/2,softening} < 1$ min) were classified as fast

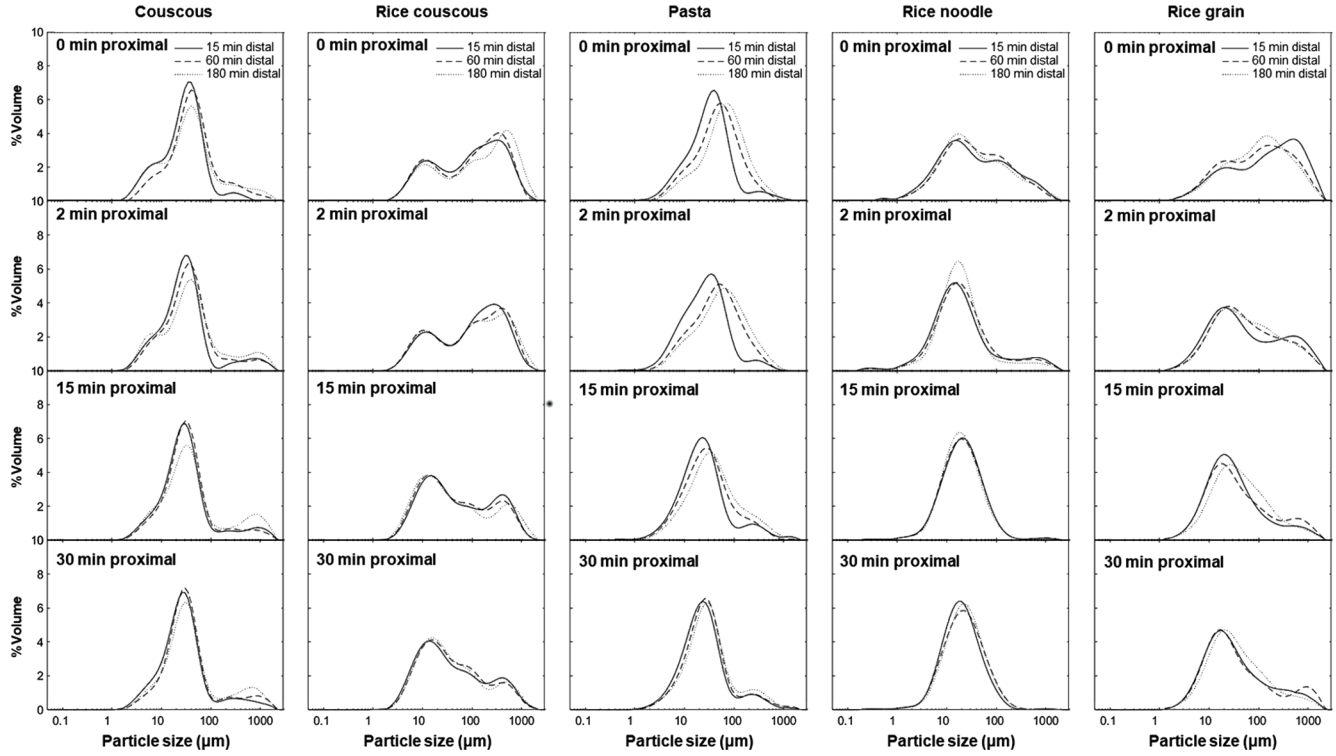

Fig. 5. Particle size distribution (PSD) of the liquid and suspended solid fractions of digesta at different proximal phase durations, over 15 min (——), 60 min (- - -), or 180 min (···) distal phase, established by averaging the PSD data of three replicates. One figure corresponds to one food type and proximal phase duration. Figures within the same column represent data for one type of food. Individual PSD curves with error shades to indicate the range of the distribution are given in Figure S9 to S13.

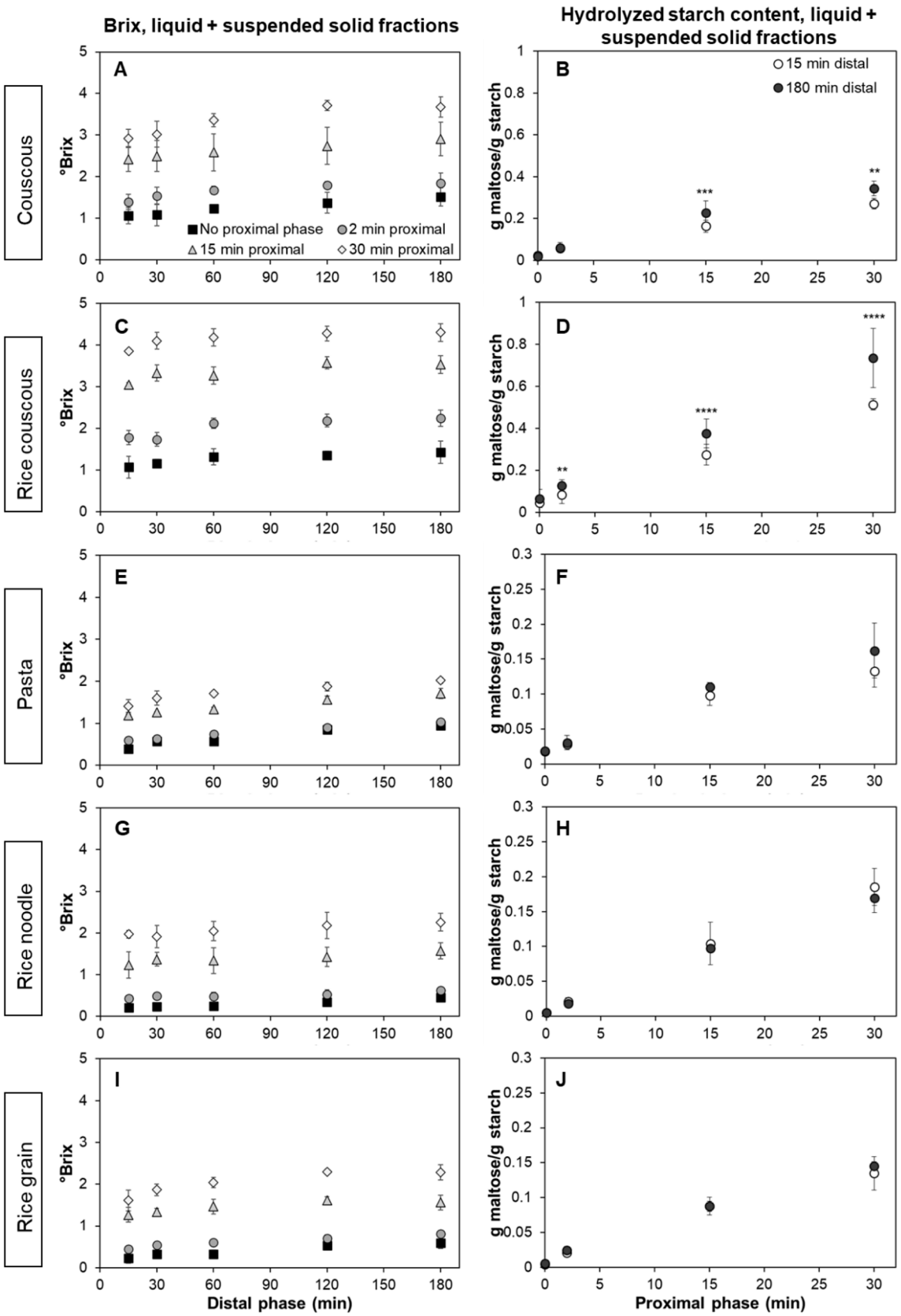

Fig. 6. Brix profiles during the distal phase, after 0 min (■), 2 min (●), 15 min (▲), or 30 min (◊) proximal phase and hydrolyzed starch content during the proximal phase after 15 min (○) or 180 min (●) distal phase. Figures within the same row correspond to one type of food: couscous (A-B), rice couscous (C-D), pasta (E-F), rice noodle (G-H), and rice grain (I-J). Values are shown as mean ± SD (n = 3 for each data point); error bars are too small to be seen for some samples. For hydrolyzed starch content of one food type, significantly different values between 15 and 180-min distal phase at one proximal phase duration are indicated by asterisks (*: $p < 0.05$, **: $p < 0.01$, ***: $p < 0.001$, ****: $p < 0.0001$).

softening, rice noodle ($t_{1/2,softening} \approx 120$ min) as intermediate softening, and rice grain and pasta ($t_{1/2,softening} > 180$ min) as slow softening (Drechsler & Bornhorst, 2018; Swackhamer, Doan, & Bornhorst, 2022).

The faster softening rate of agglomerated products compared to the three other foods might be attributed to their different particle size. Previous *in vitro* gastrointestinal studies using solid and semi-solid starch-based products reported that the rate and extent of starch digestion by α-amylase increased with smaller initial particle size of the products (Abhilasha, Kaur, Monro, Hardacre, & Singh, 2021; Mandalari et al., 2018; Tamura, Okazaki, Kumagai, & Ogawa, 2017). Gao et al. (2021) reported that smaller initial particle size of bread subjected to *in vitro* oral processing significantly decreased the bolus hardness.

The different softening rates during prolonged incubation with α-amylase might also be related to different processing methods of the raw materials to obtain the different physical structures (Bornhorst, Hivert, & Singh, 2014; Vanhatalo et al., 2021), which affected the presence of barrier to starch hydrolysis, such as microstructural arrangements of starch in the foods and the porosity of the food structure (Gao et al., 2021). The $t_{1/2,softening}$ of rice grain and noodle products that were longer than the proximal phase duration tested in the current study ($t_{1/2,softening}$ of 123.5, 355.9, or 541.8 min for rice noodle, rice grain, and pasta, respectively) suggests that the physical structure and microstructure of these foods limited starch hydrolysis during the 30 min proximal phase considered in this study (Dhital, Warren, Butterworth, Ellis, & Gidley, 2017; Hasjim, Lavau, Gidley, & Gilbert, 2010).

Starch hydrolysis by α-amylase that occurred during the proximal phase was hypothesized to generate soluble and/or small particles. This was supported by the increased proportion of particles ≤ 4 mm^2 (measured via image analysis) with longer proximal phase in the whole digesta mixture ("-" distal phase bar graphs in Fig. 2B-F), which was observed in all foods. These particles likely leached into the SGF during the distal phase as soon as SGF was added, which were identified as the suspended solid fraction after separation of the large solids from the digestion mixture. Moreover, significant reduction in the asymptotes of both W_t/W_0 and DM_t/DM_0 with longer proximal phase in the proximal–distal digestion (Fig. 3, Table 2) implied more leaching of particles ≤ 4 mm^2 from the food matrices due to prolonged proximal phase, even in the absence of mechanical forces. The 4-mm^2 limit for definition of the small particle fraction was selected based on the aperture of the mesh used to separate the solid fraction of digesta (1-mm × 2-mm; assuming circular-shaped area, the theoretical projected area was rounded up to 4 mm^2 for practicality). These observations suggest that starch hydrolysis during the proximal phase generated particles <2 mm (suspended and soluble solids), thus playing an important role in aiding the overall breakdown of solid foods during gastric digestion.

4.2. Changes to solid digesta fraction during the distal phase

Previous *in vitro* static gastric digestion studies without an extended proximal phase have associated macro- and microstructural changes in food particles during gastric digestion with the diffusion of gastric fluid components (acid, moisture, and enzymes) into the food matrix (Kong et al., 2011; Mennah-Govela & Bornhorst, 2016a; Somaratne et al., 2019). In the current study, the diffusion of SGF into the food matrices during the distal phase was observed in the increasing W_t/W_0 in rice grain and noodle products (Fig. 3) and increasing moisture uptake of digesta solid fraction of all foods (Fig. 4). This increased moisture uptake was a result of increased moisture diffusion, which may have been enhanced by the diffusion of acid and pepsin that changed the food matrices (Mennah-Govela & Bornhorst, 2016b; Somaratne et al., 2019), although the diffusion of acid and pepsin was not directly measured here. Increased moisture content or uptake correlates with decreased rheological and/or textural properties of *in vivo* and *in vitro* digesta (Bornhorst, Ferrua, Rutherfurd, Heldman, & Singh, 2013; Martens et al., 2019; Nadia, Olenskyj, et al., 2021; Swackhamer et al., 2022). Due to the increased moisture uptake, coupled with the action of acid and digestive enzymes on the food matrix, the solid fraction of digesta underwent softening during the distal phase digestion, regardless of the preceding proximal phase duration (Fig. 4).

Although all foods underwent softening during the distal phase, variations in the model fit parameters (Eqn. (2)) to each replicate of the softening kinetic curves of the solid fraction (Figure S2) were observed; this resulted in limited significant differences between model fit parameters across proximal phase and food types (Table 2). Consequently, prolonged proximal phase did not appear to enhance the softening process of the foods during the distal phase. These variations may have resulted from small differences in the removal of free liquid from the digesta mixture during separation of the solid fraction, as previous studies have found that certain amount of liquid is needed to fill the void space between food particles when bulk compression method is used (Drechsler & Bornhorst, 2018).

In determining the softening kinetics ($t_{1/2,softening}$) of the solid digesta fraction in the proximal–distal digestion, food type was a key factor ($p < 0.001$). As there were no significant differences in the $t_{1/2,softening}$ for all foods across proximal phase times and previous studies on food softening during digestion have not considered an extended proximal phase, the softening rates during the distal phase are more representative to be compared at no proximal phase (Table 2). The agglomerated products ($t_{1/2,softening} < 60$ min) were fast softening, rice grain was intermediate softening ($t_{1/2,softening} \approx 150$ min), and the noodle products ($t_{1/2,softening} > 180$ min) were slow softening (Swackhamer et al., 2022). These values were not directly comparable to the *in vivo* limiting $t_{1/2,softening}$ of similar products in swine distal stomach digesta ($t_{1/2,softening}$ of agglomerated products <2 min, rice noodle ~17 min, rice grain ~80 min, and pasta ~101 min), possibly due to the absence of mechanical breakdown from mastication and gastric wall contractions – especially in rice grain and noodle products that had $t_{1/2,softening} \geq 150$ min (similar to or longer than the distal phase tested), as well as physiological response that affected material emptying and variations in dilution with gastric secretions observed *in vivo* (Nadia, Olenskyj, et al., 2021). However, the trend across the products was comparable to the trend observed in that *in vivo* study, with the exception of rice noodle, which had fast softening *in vivo* compared to slow softening *in vitro*. Compared to an *in vitro* gastric digestion study that used similar foods with a single compression method (medium grain white rice, $t_{1/2,softening}$ ~38 min; orzo pasta, $t_{1/2,softening}$ ~71 min), the values found here were different, although the trend was consistent, where the rice softened faster than pasta (Drechsler & Bornhorst, 2018). The lack of similarity between the $t_{1/2,softening}$ reported here and those reported by Drechsler and Bornhorst (2018) may be associated with different product specifications (e.g. amylose content due to different grain variety) and geometries (size and shape of the food particles) that affect the diffusivity of acid into the food matrix (Mennah-Govela, Bornhorst, & Singh, 2015) and direction of gastric fluid diffusion into the food particles.

With minimum mechanical force (except gentle shaking) during the distal phase in this study, minimum particle breakdown was expected. However, a significant decrease in DM_t/DM_0 towards an asymptote value during the distal phase was observed in rice couscous at all proximal phase times, and in couscous at proximal phase ≥ 2 min (Fig. 3B,D). This may suggest additional breakdown of the agglomerated products due to dissolution by SGF in the distal phase that formed digesta with cohesive, slurry-like consistency; as shown by the decreasing particles between 10 and 100 mm^2 with longer distal phase and the prevalence of particles ≤ 4 mm^2 in the solid fraction despite the sieving process following the distal phase (Fig. 2B-D). In the non-agglomerated foods, reduction in DM_t/DM_0 during the distal phase was limited (Fig. 3F,H,J), suggesting minimal generation of particles ≤ 4 mm^2. In noodle products, the majority (>85%) of the particles remained >100 mm^2 throughout the distal phase, indicating no notable breakdown, although the slightly decreasing proportion of particles >100 mm^2 might reflect surface damages of the noodle (Drechsler & Ferrua,

2016). However, fragmentation was observed in rice grain (Figure S14) at prolonged proximal phase (30 min) or distal phase (180 min), together with significant decrease in the x_{50} of rice grain digesta and the decreasing proportion of particles between 10 and 100 mm^2 with longer proximal and/or distal phase (Table 3, S4-S5). The fragmentation that was only observed in rice grain, but not the noodle products, might be related to their different microstructure and geometries (Fig. 7, see Section 4.4 for further discussion on this topic), and should be investigated in future studies.

4.3. Changes to liquid and suspended solid fractions of digesta due to the proximal and distal phases

Together with the excess liquid, most particles $\leq$4 mm^2 (in the form of soluble and suspended solids) were separated from the large particles by the end of proximal–distal digestion to simulate gastric sieving. The liquid-suspended solid mixture was expected to represent the fractions that would be prioritized for gastric emptying during gastric digestion *in vivo*. As these digesta fractions were smaller in size than the solid digesta fraction, they were expected to undergo more changes in particle size and hydrolysis due to the proximal and distal phases.

In the Mastersizer measurement, the distinct locations of the first peak at 15 min distal phase (Fig. 5) between the wheat- and rice-based foods matched with the diameter of Durum wheat starch granules (20–25 μm) and rice starch granules (3–15 μm) (Abecassis, Cuq, Boggini, & Namoune, 2012; Ramadoss et al., 2019). The %volume of particles in this first peak generally increased with longer proximal phase, indicating more starch particles were released to the SGF during the proximal phase. While no significant differences between rice- and wheat-based foods were observed in the particle size parameters of solid digesta fraction, possibly due to the more significant contribution of the food macrostructure in the bulk of the solids, the effect of starch source was observed in the liquid and suspended solid fractions of digesta. Changes in the D[4,3] and D[3,2] were more notable in the proximal phase for rice-based foods and in the distal phase for wheat-based foods (Table 3) – as also seen in their distinct PSD profiles (Fig. 5). This is possibly linked to their hydrolysis characteristics; an *in vitro* study using native starches reported that hydrolysis by α-amylase was higher in rice starch, whereas hydrolysis by HCl was higher in wheat starch (V. Singh & Ali, 2006). The effect of starch source that was observed in the liquid and suspended solid fractions possibly suggests that starch properties govern the digestion behaviour when a macrostructural barrier is absent.

°Brix in the liquid-suspended solid mixture increased significantly with longer proximal phase time (Fig. 6), which suggested more soluble solids were released during the proximal phase. Increasing °Brix during the distal phase indicated solubilization of particles in the SGF. Although the differences in the °Brix profile between foods and proximal phase durations were clear in the current study, future studies can consider the application of mathematical model (as applied to the DM_t/DM_0, W_t/W_0, and H_t/H_0 profile) to enable quantitative comparison across treatments. Aligned with the trend in the softening rate in both proximal and proximal–distal digestion, hydrolyzed starch content in the liquid-suspended solid mixture was higher for agglomerated products after

Table 3
Selected particle size parameters of the solid digesta fraction measured using image analysis after all proximal phase times followed by 30 or 180 min distal phase. Values are shown as mean ± SD (n = 3 for each food × proximal × distal phase combination). Moisture content of each sample was used to calculate the number of particles per gram dry matter (particles/g DM). Significantly different values between distal phase duration for one type of food are indicated with superscripts ab. Significantly different values between proximal phase durations for one type of food are indicated with superscript zyxw ($p < 0.05$). Additional particle size parameters can be found in Table S8.

Food	Distal phase (min)	Proximal phase (min)			
		0	2	15	30
x_{50} (mm^2)					
Couscous	30	2.20 ± 0.29	3.39 ± 2.05^{a}	2.94 ± 1.22^{a}	2.03 ± 0.60
	180	1.94 ± 0.10^{z}	2.33 ± 1.22^{b,z}	1.80 ± 0.73^{b,y}	1.76 ± 0.59^{zy}
Rice couscous	30	2.81 ± 1.26	2.71 ± 1.10	2.50 ± 1.09	2.84 ± 1.25
	180	2.84 ± 0.33	2.61 ± 0.79	3.10 ± 0.64	2.47 ± 0.55
Pasta	30	269.69 ± 46.17	291.70 ± 35.52	255.75 ± 55.39	231.84 ± 92.96
	180	211.81 ± 54.06	283.73 ± 77.96	202.52 ± 68.75	232.35 ± 26.04
Rice noodle	30	203.71 ± 55.76	207.94 ± 46.49	204.26 ± 42.47	233.42 ± 15.22
	180	224.47 ± 51.25	215.77 ± 31.84	208.49 ± 71.17	217.59 ± 34.17
Rice grain	30	40.97 ± 6.65^{a,z}	45.75 ± 18.66^{a,z}	24.70 ± 3.86^{a,y}	23.22 ± 7.03^{a,y}
	180	19.75 ± 6.19^{b,z}	21.63 ± 7.54^{b,z}	20.47 ± 2.91^{b,z}	16.51 ± 4.89^{b,y}
Particles/g DM*					
Couscous	30	4227 ± 1641	3762 ± 1373	5311 ± 1621	7614 ± 1265
	180	4478 ± 800	4649 ± 673	7315 ± 1784	8662 ± 2104
Rice couscous	30	5467 ± 1618	5737 ± 1751	4984 ± 1797	4885 ± 2314
	180	6169 ± 1967	5998 ± 3190	4214 ± 2441	4342 ± 1338
Pasta	30	69 ± 42^{b}	35 ± 11^{b}	39 ± 9^{b}	70 ± 44
	180	120 ± 42^{a}	148 ± 95^{a}	133 ± 35^{a}	111 ± 79
Rice noodle	30	49 ± 14^{b}	59 ± 18^{b}	60 ± 5	91 ± 14
	180	100 ± 53^{a}	114 ± 50^{a}	102 ± 51	130 ± 76
Rice grain	30	282 ± 120	385 ± 311	472 ± 264	633 ± 197
	180	484 ± 309	621 ± 493	580 ± 86	490 ± 73
Average area (mm^2)/particle					
Couscous	30	1.30 ± 0.13	1.78 ± 0.88	1.72 ± 0.64^{a}	1.26 ± 0.33
	180	1.13 ± 0.11	1.34 ± 0.59	1.17 ± 0.38^{b}	1.15 ± 0.31
Rice couscous	30	1.20 ± 0.33	1.12 ± 0.28	1.13 ± 0.36	1.19 ± 0.45
	180	1.27 ± 0.07	1.20 ± 0.28	1.42 ± 0.23	1.19 ± 0.29
Pasta	30	56.69 ± 34.52^{a,zy}	88.79 ± 30.77^{a,zy}	71.92 ± 4.78^{a,z}	51.22 ± 26.25^{a,y}
	180	23.19 ± 6.36^{b}	29.8 ± 22.6^{b}	22.91 ± 6.73^{b}	36.22 ± 15.32^{b}
Rice noodle	30	87.05 ± 24.84^{a}	72.60 ± 5.14^{a}	78.40 ± 13.39^{a}	68.31 ± 6.51
	180	58.66 ± 30.29^{b}	46.79 ± 8.51^{b}	57.49 ± 9.13^{b}	59.20 ± 25.95
Rice grain	30	8.23 ± 0.70^{a}	8.95 ± 2.99^{a}	8.01 ± 4.06^{a}	6.25 ± 2.90
	180	4.82 ± 2.21^{b}	5.08 ± 2.16^{b}	6.66 ± 1.12^{b}	6.63 ± 1.55

*The values of particles/g DM are presented as integers because they represent individual particles present in each gram of digesta dry matter.

Table 4
Volume mean diameter (D[4,3]) and surface area mean diameter (D[3,2] of the liquid and suspended solid digesta fractions measured using the Mastersizer. Values are mean ± SD (n = 3 for each food × proximal × distal phase combination). Significantly different values between distal phase duration for one type of food are indicated with abcd superscript. Significantly different values between proximal phase for one food type within the same distal phase duration are indicated with zyxw superscript ($p < 0.05$).

Food	Proximal phase (min)	D[4,3] (μm) Distal phase (min)					D[3,2] (μm) Distal phase (min)				
		15	30	60	120	180	15	30	60	120	180
Couscous	0	42.6 ± 11.3^{c,y}	57.5 ± 13.1^{bc}	73.0 ± 25.3^{ab}	92.9 ± 35.2^{a}	103.6 ± 33.4^{a}	16.0 ± 3.7	16.5 ± 3.4	19.4 ± 3.4	19.7 ± 1.4	18.4 ± 3.1
	2	90.3 ± 65.5^{z}	65.6 ± 4.2	93.8 ± 16.5	105.5 ± 36.4	132.3 ± 69.1	16.0 ± 3.4	15.8 ± 3.2	17.8 ± 2.4	19.0 ± 2.1	19.3 ± 3.1
	15	94.7 ± 54.7^{ab,z}	94.3 ± 41.5^{ab}	85.2 ± 41.5^{a}	130.8 ± 63.5^{ab}	155.5 ± 51.2^{a}	16.9 ± 3.3	17.4 ± 3.1	18.0 ± 2.1	20.0 ± 2.9	19.2 ± 2.4
	30	74. 8 ± 22.9^{zy}	85.6 ± 36.1	105.2 ± 68.0	121.7 ± 46.7	129.4 ± 28.0	16.4 ± 2.6	17.6 ± 3.6	18.7 ± 2.2	18.7 ± 2.7	19.2 ± 2.3
Rice couscous	0	198.6 ± 71.4	212.3 ± 66.7	203.3 ± 37.4	208.2 ± 34.4^{zy}	286.3 ± 36.6^{z}	24.3 ± 3.5^{zy}	24.3 ± 2.2^{z}	25.1 ± 3.3^{z}	24.5 ± 3.9^{z}	27.3 ± 3.2^{z}
	2	199.5 ± 43.3	210.8 ± 47.4	214.7 ± 43.2	235.8 ± 72.0^{z}	237.3 ± 100.2^{zy}	25.2 ± 2.7^{z}	24.1 ± 1.5^{z}	23.8 ± 4.3^{z}	26.8 ± 4.6^{z}	25.9 ± 7.2^{z}
	15	153.4 ± 20.7	181.8 ± 71.3	141.3 ± 33.2	150.4 ± 33.3^{zy}	165.1 ± 61.6^{zy}	18.6 ± 2.7^{y}	18.2 ± 4.0^{y}	17.2 ± 3.0^{y}	17.5 ± 3.8^{y}	16.4 ± 4. 7^{y}
	30	126.6 ± 60.4	131.5 ± 64.0	115.0 ± 21.6	113.3 ± 24.1^{y}	125. 7 ± 30.8^{y}	15.1 ± 2.9^{b,x}	17.2 ± 5.2^{ab,y}	17.4 ± 5.0^{ab,y}	16.6 ± 3.2^{ab,y}	17.4 ± 5.1^{a,y}
Pasta	0	58.2 ± 8.1^{ab}	55.7 ± 10.2^{b}	71.7 ± 16.5^{ab}	82.5 ± 15.2^{ab}	97.9 ± 20.6^{a}	16.5 ± 2.9^{d,z}	19.4 ± 2.2 ^{cd,z}	23.5 ± 1.4^{bc,z}	27.1 ± 3.0^{ab,z}	30.7 ± 0.8^{a,z}
	2	46.7 ± 2.7^{b}	60. 2 ± 6.8^{ab}	74.9 ± 14.1^{ab}	87.7 ± 15.8^{a}	95.2 ± 8.7^{a}	13.6 ± 2.2^{c,zy}	17.9 ± 0.6^{b,zy}	21.0 ± 2.9^{ab,z}	24.6 ± 1.5^{a,z}	25.4 ± 1.3^{a,z}
	15	60.8 ± 21.8	51.0 ± 8.7	58.4 ± 9.2	77.9 ± 4.8	83.0 ± 8.5	12.6 ± 2.0^{c,y}	13.7 ± 1.7^{bc,y}	15.1 ± 1. 5^{abc,y}	17.2 ± 1.5^{ab,y}	18.8 ± 0.9^{a,y}
	30	55.0 ± 14.2	58.7 ± 18.5	66.4 ± 13.9	69.0 ± 13. 7	72. 6 ± 15. 7	13.9 ± 1.6^{zy}	14.6 ± 1.7^{y}	15.9 ± 1.9^{y}	16.9 ± 2.0^{y}	17.2 ± 2.0^{y}
Rice noodle	0	113.6 ± 29.2^{z}	99.6 ± 42.1^{z}	104.1 ± 36.9^{z}	116.4 ± 34.6^{z}	111.3 ± 58.7^{z}	11.3 ± 5.1^{z}	12.8 ± 7.7^{z}	13.5 ± 6.6^{z}	13.5 ± 6.0^{y}	12.7 ± 7.8^{z}
	2	84.2 ± 13.1^{z}	70.3 ± 28.8^{z}	77.0 ± 43.1^{zy}	77.7 ± 35.0^{z}	60.1 ± 15.1^{y}	8.3 ± 5.5^{y}	8.3 ± 5.2^{y}	10.1 ± 7.8^{y}	8.4 ± 5.4^{y}	9.2 ± 3.5^{y}
	15	35.9 ± 9.9^{y}	25.7 ± 6.5^{y}	37.7 ± 13.7^{yx}	32.7 ± 11.4^{y}	32.5 ± 7.1^{y}	12.2 ± 6.8^{z}	10.3 ± 4.5^{z}	12.5 ± 7.5^{z}	12.3 ± 7.5^{z}	11.4 ± 5.9^{z}
	30	29.7 ± 6.9^{y}	27.0 ± 8.8^{y}	33.5 ± 12.8^{x}	30.6 ± 12.8^{y}	33.5 ± 8.8^{y}	11.7 ± 5.3^{z}	12.1 ± 5.2^{z}	13.8 ± 8.1^{z}	13. 5 ± 7.8^{z}	14.1 ± 6.5^{z}
Rice grain	0	302.9 ± 77.7^{z}	277.0 ± 24.1^{z}	223.0 ± 10.3	211.9 ± 31.5^{z}	209.6 ± 69.8^{z}	34.0 ± 8.5^{z}	32.0 ± 6.8^{z}	27.9 ± 4.3^{z}	29.3 ± 5.4^{z}	33.3 ± 9.7^{z}
	2	138.2 ± 27.3^{y}	178.9 ± 56.9^{zy}	158.9 ± 30.9	162.4 ± 29.0^{z}	158.7 ± 35.9^{zy}	17.0 ± 4.3^{y}	18.2 ± 2.7^{y}	20.8 ± 3.8^{z}	22.1 ± 1.5^{z}	21.8 ± 4.5^{zy}
	15	96. 9 ± 49.4^{y}	91.9 ± 36.5^{x}	130.0 ± 58.2	128.3 ± 50.5^{zy}	106.3 ± 34.2^{y}	15.6 ± 2.7^{y}	15.1 ± 1.5^{x}	16.5 ± 3.7^{y}	17.2 ± 2.8^{y}	19.1 ± 1.0^{yx}
	30	115.0 ± 34.7^{ab,y}	124.8 ± 40.5^{ab,yx}	149.3 ± 35.2^{a}	78.1 ± 1.2^{b,y}	100.9 ± 20.9^{ab,y}	15.1 ± 2.1^{y}	15.7 ± 3.1^{x}	15.5 ± 2.4^{y}	13.6 ± 1.2^{y}	16.7 ± 1.1^{x}

any proximal phase duration after 15 min distal phase (Fig. 6), indicating the agglomerated products were more prone to starch hydrolysis by α-amylase. After a distal phase duration of 180 min, there was a significant increase ($p < 0.01$) in starch hydrolysis observed in the agglomerated products at proximal phase ≥15 min, which was not observed in the non-agglomerated products. This agrees with a study that reported amylolysis of a native waxy rice starch dispersion followed by acid hydrolysis at human physiological temperature increased the degree of hydrolysis of the starch (Li et al., 2013). The significantly increasing hydrolysis that was only observed in the agglomerated products implies that acid hydrolysis during gastric digestion might enhance starch hydrolysis, but only if amylolysis and acid diffusion are not limited by a microstructural or macrostructural barrier. Together with the trends in the Mastersizer measurement, the difference in the hydrolyzed starch content of the foods due to proximal–distal gastric digestion are expected to impact the starch digestibility of these food products during small intestinal digestion and merit future investigation.

4.4. Food structure and geometry influence breakdown mechanisms during proximal and distal phases of gastric digestion

Changes that occur during the proximal and distal phase of gastric digestion have been shown to be influenced by food structure, as also observed in an *in vivo* study (growing pig model) using the same food products (Nadia, Olenskyj, et al., 2021), especially in terms of their softening behavior. The fast-softening behavior of the agglomerated products in both *in vivo* digestion studied by Nadia, Olenskyj, et al. (2021) and *in vitro* digestion studied here, as well as their high hydrolyzed starch content during the proximal–distal *in vitro* digestion, can be associated with their small initial particle size ($1 < d \leq 2$ mm), porous microstructure (Hafsa et al., 2014), and their spherical geometry that provides the largest surface area per volume ratio (SA/V) among the foods studied (Fig. 7). These factors enabled digestive fluid components to diffuse from the surface into the internal structure of their matrices (Dhital et al., 2017), resulting in the dissociation and dissolution of the agglomerates (Barkouti, Delalonde, Rondet, & Ruiz, 2014) in SGF, which resulted in a fast softening rate in the distal phase (Bornhorst, Ferrua, & Singh, 2015).

In rice grain, the access of digestive fluid components into the internal part of the rice kernel was physically limited by the protein matrix and cell walls encapsulating the starch granules (Dhital, Brennan, & Gidley, 2019; Tamura, Singh, Kaur, & Ogawa, 2016). Since the rice grains had a cylindrical-like geometry, the diffusion of digestive fluids occurred mainly in the radial direction (the shortest dimension; Fig. 7). At early durations, proximal and distal phases were thought to cause

Structure	Agglomerates	Grain	Noodle
Before digestion Matrix entrapping starch particles Starch particles in the matrix	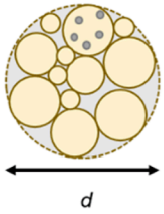 d = 1 - 2 mm	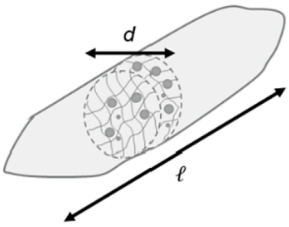 d = ~2 mm, ℓ = ~10 mm	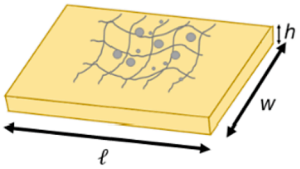 w = ~7 mm, ℓ = ~15 - 18 mm, h = 1 - 1.5 mm
Estimated surface area per volume (SA/V, mm^{-1})	3 – 6	2.2 – 2.3	0.5 – 0.7
Direction of digestive fluid diffusion	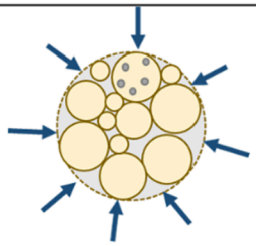 Radial	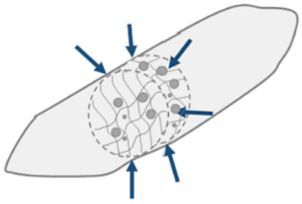 Radial	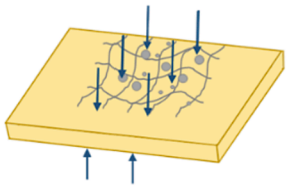 Axial
Main breakdown mechanism due to digestive fluid diffusion	Dissolution	Surface erosion, fragmentation (at later duration)	Surface erosion
Factors limiting the release of starch particles	Agglomerate diameter, agglomerate strength	Macrostructural breakdown, matrix entrapping the starch particles	Macrostructural breakdown, matrix entrapping the starch particles

Fig. 7. Hypothesized breakdown mechanisms of the food structures due to digestive fluid diffusion during proximal and distal phase in the current study, as affected by food geometry and the direction of digestive fluid diffusion into the food matrix. The surface area to volume (SA/V) ratio was estimated from the characteristic dimensions of each food (*d*: diameter, *ℓ*: length, *w*: width, *h*: thickness). Representative starch particles and selected region showing the food matrix are shown to reflect the entrapment of starch particles in the food structure. Factors limiting the release of starch granules from the structure are also proposed based on the main breakdown mechanisms observed for each type of food structure.

surface erosion, as observed in the increasing particles $\leq$4 mm^2 in the digesta compared to the undigested rice grain (Fig. 2F). Prolonged duration of proximal phase (30 min) or distal phase (180 min) might have allowed further penetration of α-amylase and SGF components into the internal structure, causing fragmentation in the radial direction (Figure S14). This might be due to the breakage and dissolution of cell walls, as previously observed during prolonged static soaking of rice kernel (Wu et al., 2017), sweet potatoes (Mennah-Govela & Bornhorst, 2016b; Somaratne et al., 2020), and apples (Olenskyj, Donis-González, & Bornhorst, 2020) in SGF. Despite its cylindrical-like geometry (SA/V ~4 times the noodle products) that resulted in physical fragmentation of the rice kernels, the hydrolyzed starch content of rice grain was similar to that of pasta and slightly lower than that of rice noodle. This suggests the microstructure of rice grain limited the breakdown and hydrolysis related to diffusion of digestive fluids, and that breakdown of the macrostructure is required to release starch from the matrix. Fragmentation that occurred due to prolonged proximal or distal phase and the slow hydrolysis of rice grain may explain its similar $t_{1/2,softening}$ in the proximal and distal *in vivo* gastric digesta, longer *in vivo* $t_{1/2,softening}$ compared to rice noodle, and shorter *in vivo* $t_{1/2,softening}$ compared to pasta (Nadia, Olenskyj, et al., 2021).

In the noodle products, the diffusion of α-amylase and SGF components into the noodle pieces was thought to mainly take place in the direction of the thickness (the shortest dimension; Fig. 7) due to their slab geometry. Although their thickness was similar to the diameter of the agglomerated products (~1 and 1.5 mm), the $t_{1/2,softening}$ in both proximal and proximal–distal digestion were longer than the agglomerated products. This implies that the microstructure of the noodles limited the diffusion of digestive fluid components, thus only allowed the diffusion to occur gradually from the outer layer of the shortest dimension to the center, as observed in a microstructural observation study on the diffusion of α-amylase and SGF to intact piece of pasta (Zou, Sissons, Gidley, Gilbert, & Warren, 2015). It was hypothesized that the breakdown mechanisms in the noodle products were surface erosion either by α-amylase in the proximal phase (Dhital et al., 2017), or by acid and pepsin in the SGF (Swackhamer et al., 2022). With the minimum breakdown by only biochemical changes, macrostructural breakdown of the noodle structure is required to enhance the release of starch from the matrix (Fig. 7). Starch source and microstructural differences between rice noodle (solubilized starch gel with no physical barrier encapsulating the starch) and pasta (starch particles entrapped in starch-protein matrix) possibly affected the rate of diffusion and surface erosion by digestive fluids (Klinmalai, Hagiwara, Sakiyama, & Ratanasumawong, 2017; Zou et al., 2015), resulting in different softening kinetics between these foods in the proximal and proximal–distal digestion (Fig. 2A, Table 2). The microstructural differences may also explain the difference in the *in vivo* $t_{1/2,softening}$ of pasta and rice noodle in the proximal and distal stomach, where pasta had faster softening in the

distal stomach, whereas rice noodle had faster softening in the proximal stomach (Nadia, Olenskyj, et al., 2021). The slower starch hydrolysis of pasta compared to noodle during the proximal phase at both 15- and 180-min distal phase (Fig. 6) may explain the longer *in vivo* $t_{1/2,softening}$ of pasta compared to rice noodle (Nadia, Olenskyj, et al., 2021).

It is noteworthy that geometrical differences between the foods that were considered to affect the diffusion of digestive fluids are comparable to diffusion-controlled drug delivery systems (Siepmann & Siepmann, 2012). The different geometries of the foods led to different SA/V, where the SA/V of agglomerated products > rice grain > noodle products. Higher SA/V was reported to increase the rate of drug release in a study of controlled-release tablets (Reynolds, Mitchell, & Balwinski, 2002). However, the discrepancy in rice grain that fragmented during prolonged proximal or distal phase, but had similar starch hydrolysis to noodle products implied that food microstructure also influenced the mechanisms of food breakdown during the proximal and distal gastric digestion (Fig. 7). Future studies should include microstructural observations and measurements to explore these hypotheses. Since food structure and starch digestibility can be impacted by the preparation method, including cooking duration (Pellegrini, Vittadini, & Fogliano, 2020; J. Singh, Dartois, & Kaur, 2010), separate studies can be done to elucidate the effect of preparation method of each food in the current study on food breakdown during gastric digestion, as standardized cooking methods were used to prepare the foods in the current study. Additionally, the breakdown mechanisms may be affected by mastication and gastric contraction forces (i.e., macrostructural breakdown), which were outside the scope of the present study.

5. Conclusions

The proximal gastric phase, where the exposure to α-amylase is extended, is often not considered in gastric digestion studies. However, this work demonstrated that the proximal phase affected the properties of food particles during the distal phase of gastric digestion, through the generation and leaching of small particles (<2 mm) via starch hydrolysis. Through softening kinetics and solid retention kinetics modelling, the difference between the proximal and distal phase was able to be identified quantitatively, suggesting empirical modelling can be applied to analyze and interpret large, complex datasets from digestion studies. The distal phase contributed to increased gastric fluid uptake into the food particles, which resulted in softening. The prolonged proximal phase preceding the distal phase did not enhance softening during the distal phase. However, the proximal phase preceding the distal phase enhanced the starch hydrolysis of leached particles in agglomerated products after 180 min distal phase, suggesting that acid hydrolysis might enhance starch hydrolysis initiated by α-amylase, but only in the absence of micro- and macrostructural barriers in the food matrix.

Food structure and geometry (size and shape, which define its SA/V) influenced the breakdown mechanisms during proximal and distal gastric digestion, in the absence of mechanical forces. The smaller initial size, porous microstructure, and spherical shape of agglomerated products might be associated with their fast-softening behavior during gastric digestion. The larger initial size of rice grain and noodle products, combined with the presence of more barriers to enzyme diffusion in their microstructure and their shapes, might be associated with their intermediate- to slow-softening behavior during gastric digestion. In addition, starch sources of these products were also found to affect the properties of the leached particles during the proximal and distal phase, although the effect was not as apparent as their physical structure. Overall, the current study demonstrated that food structure is crucial in determining breakdown mechanisms in the proximal and distal phases of gastric digestion. The impact of factors affecting food structure (e.g., preparation method) on the breakdown mechanisms identified here should be investigated in future studies for a broader application of the current findings.

CRediT authorship contribution statement

Joanna Nadia: Conceptualization, Methodology, Software, Investigation, Visualization, Writing – original draft. **John Bronlund:** Conceptualization, Writing – review & editing. **Harjinder Singh:** Conceptualization, Writing – review & editing, Funding acquisition. **R. Paul Singh:** Conceptualization, Writing – review & editing. **Gail M. Bornhorst:** Conceptualization, Methodology, Writing – review & editing, Supervision.

Declaration of Competing Interest

The authors declare that they have no known competing financial interests or personal relationships that could have appeared to influence the work reported in this paper.

Acknowledgments

Joanna Nadia gratefully acknowledges the Riddet Institute (Massey University, Palmerston North, New Zealand) for the financial support for her doctoral scholarship (grant number: Centre of Research Excellence – Riddet Institute, ref: A914656). The authors thank Dr. Parthasarathi Subramanian for his assistance in particle size measurement using Mastersizer.

Appendix A. Supplementary data

Supplementary data to this article can be found online at https://doi.org/10.1016/j.foodres.2022.111270.

References

Abecassis, J., Cuq, B., Boggini, G., & Namoune, H. (2012). Other traditional durum-derived products. In M. Sissons, J. Abecassis, B. Marchylo, & M. Carcea (Eds.), *Durum wheat: Chemistry and technology*. AACC International: Minnesota, USA.

Abhilasha, A., Kaur, L., Monro, J., Hardacre, A., & Singh, J. (2021). Intact, kibbled, and cut wheat grains: Physico-chemical, microstructural characteristics and gastro-small intestinal digestion in vitro. *Starch-. Stärke, 73*(7-8), 2000267.

Angelidis, G., Protonotariou, S., Mandala, I., & Rosell, C. M. (2016). Jet milling effect on wheat flour characteristics and starch hydrolysis. *Journal of Food Science and Technology, 53*(1), 784–791.

Barkouti, A., Delalonde, M., Rondet, E., & Ruiz, T. (2014). Structuration of wheat powder by wet agglomeration: Case of size association mechanism. *Powder Technology, 252*, 8–13.

Bornhorst, G. M., Ferrua, M. J., Rutherfurd, S. M., Heldman, D. R., & Singh, R. P. (2013). Rheological properties and textural attributes of cooked brown and white rice during gastric digestion in vivo. *Food Biophysics, 8*(2), 137–150.

Bornhorst, G. M., Ferrua, M. J., & Singh, R. P. (2015). A proposed food breakdown classification system to predict food behavior during gastric digestion. *Journal of Food Science, 80*(5), R924–R934.

Bornhorst, G. M., Hivert, H., & Singh, R. P. (2014). Rice bolus texture changes due to α-amylase. *LWT - Food Science and Technology, 55*(1), 27–33.

Bornhorst, G. M., Rutherfurd, S. M., Roman, M. J., Burri, B. J., Moughan, P. J., & Singh, R. P. (2014). Gastric pH distribution and mixing of soft and rigid food particles in the stomach using a dual-marker technique. *Food Biophysics, 9*(3), 292–300.

Brodkorb, A., Egger, L., Alminger, M., Alvito, P., Assuncao, R., Ballance, S., … Recio, I. (2019). INFOGEST static in vitro simulation of gastrointestinal food digestion. *Nature Protocols, 14*(4), 991–1014.

Brownlee, I. A., Gill, S., Wilcox, M. D., Pearson, J. P., & Chater, P. I. (2018). Starch digestion in the upper gastrointestinal tract of humans. *Starch-Stärke, 70*(9–10), 1700111.

Dhital, S., Brennan, C., & Gidley, M. J. (2019). Location and interactions of starches in planta: Effects on food and nutritional functionality. *Trends in Food Science & Technology, 93*, 158–166.

Dhital, S., Warren, F. J., Butterworth, P. J., Ellis, P. R., & Gidley, M. J. (2017). Mechanisms of starch digestion by α-amylase-Structural basis for kinetic properties. *Critical Reviews in Food Science and Nutrition, 57*(5), 875–892.

Drechsler, K. C., & Bornhorst, G. M. (2018). Modeling the softening of carbohydrate-based foods during simulated gastric digestion. *Journal of Food Engineering, 222*, 38–48.

Drechsler, K. C., & Ferrua, M. J. (2016). Modelling the breakdown mechanics of solid foods during gastric digestion. *Food Research International, 88*, 181–190.

Englyst, K. N., Englyst, H. N., Hudson, G. J., Cole, T. J., & Cummings, J. H. (1999). Rapidly available glucose in foods: An in vitro measurement that reflects the glycemic response. *The American Journal of Clinical Nutrition, 69*(3), 448–454.

Freitas, D., & Le Feunteun, S. (2019). Oro-gastro-intestinal digestion of starch in white bread, wheat-based and gluten-free pasta: Unveiling the contribution of human salivary α-amylase. *Food Chemistry, 274*, 566–573.
Freitas, D., Le Feunteun, S., Panouille, M., & Souchon, I. (2018). The important role of salivary alpha-amylase in the gastric digestion of wheat bread starch. *Food & Function, 9*(1), 200–208.
Gao, J., Tan, E. Y. N., Low, S. H. L., Wang, Y., Ying, J., Dong, Z., & Zhou, W. (2021). From bolus to digesta: How structural disintegration affects starch hydrolysis during oral-gastro-intestinal digestion of bread. *Journal of Food Engineering, 289*, Article 110161.
Goñi, I., Garcia-Alonso, A., & Saura-Calixto, F. (1997). A starch hydrolysis procedure to estimate glycemic index. *Nutrition Research, 17*(3), 427–437.
Hafsa, I., Cuq, B., Kim, S. J., Le Bail, A., Ruiz, T., & Chevallier, S. (2014). Description of internal microstructure of agglomerated cereal powders using X-ray microtomography to study of process–structure relationships. *Powder Technology, 256*, 512–521.
Harmsen, K. (2000). A modified mitscherlich equation for rainfed crop production in semi-arid areas: 1. Theory. *NJAS - Wageningen Journal of Life Sciences, 48*(3), 237–250.
Hasjim, J., Lavau, G. C., Gidley, M. J., & Gilbert, R. G. (2010). In vivo and in vitro starch digestion: Are current in vitro techniques adequate? *Biomacromolecules, 11*, 3600–3608.
Hoebler, C., Devaux, M. F., Karinthi, A., Belleville, C., & Barry, J. L. (2000). Particle size of solid food after human mastication and in vitro simulation of oral breakdown. *International Journal of Food Sciences and Nutrition, 51*(5), 353–366.
Hutchings, S. C., Foster, K. D., Bronlund, J. E., Lentle, R. G., Jones, J. R., & Morgenstern, M. P. (2011). Mastication of heterogeneous foods: Peanuts inside two different food matrices. *Food Quality and Preference, 22*(4), 332–339.
Klinmalai, P., Hagiwara, T., Sakiyama, T., & Ratanasumawong, S. (2017). Chitosan effects on physical properties, texture, and microstructure of flat rice noodles. *LWT - Food Science and Technology, 76*, 117–123.
Kong, F., Oztop, M. H., Singh, R. P., & McCarthy, M. J. (2011). Physical changes in white and brown rice during simulated gastric digestion. *Journal of Food Science, 76*(6), E450–E457.
Kong, F., & Singh, R. P. (2009). Modes of disintegration of solid foods in simulated gastric environment. *Food Biophysics, 4*(3), 180–190.
Li, H., Zhu, Y., Jiao, A., Zhao, J., Chen, X., Wei, B., … Tian, Y. (2013). Impact of α-amylase combined with hydrochloric acid hydrolysis on structure and digestion of waxy rice starch. *International Journal of Biological Macromolecules, 55*, 276–281.
Mandalari, G., Merali, Z., Ryden, P., Chessa, S., Bisignano, C., Barreca, D., … Waldron, K. W. (2018). *Durum* wheat particle size affects starch and protein digestion in vitro. *European Journal of Nutrition, 57*, 319–325.
Martens, B. M. J., Noorloos, M., de Vries, S., Schols, H. A., Bruininx, E., & Gerrits, W. J. J. (2019). Whole digesta properties as influenced by feed processing explain variation in gastrointestinal transit times in pigs. *British Journal of Nutrition, 122*(11), 1242–1254.
Mennah-Govela, Y. A., & Bornhorst, G. M. (2016a). Acid and moisture uptake in steamed and boiled sweet potatoes and associated structural changes during in vitro gastric digestion. *Food Research International, 88*, 247–255.
Mennah-Govela, Y. A., & Bornhorst, G. M. (2016b). Mass transport processes in orange-fleshed sweet potatoes leading to structural changes during in vitro gastric digestion. *Journal of Food Engineering, 191*, 48–57.
Mennah-Govela, Y. A., Bornhorst, G. M., & Singh, R. P. (2015). Acid diffusion into rice boluses is influenced by rice type, variety, and presence of alpha-amylase. *Journal of Food Science, 80*(2), E316–E325.
Meyer, J. H., Elashoff, J., Porter-Fink, V., Dressman, J., & Amidon, G. L. (1988). Human postprandial gastric emptying of 1-3-millimeter spheres. *Gastroenterology, 94*(6), 1315–1325.
Minekus, M., Alminger, M., Alvito, P., Ballance, S., Bohn, T., Bourlieu, C., … Brodkorb, A. (2014). A standardised static in vitro digestion method suitable for food - an international consensus. *Food & Function, 5*(6), 1113–1124.
Monro, J. A., Mishra, S., & Venn, B. (2010). Baselines representing blood glucose clearance improve in vitro prediction of the glycaemic impact of customarily consumed food quantities. *British Journal of Nutrition, 103*(2), 295–305.
Nadia, J., Bronlund, J., Singh, H., Singh, R. P., & Bornhorst, G. M. (2021). Structural breakdown of starch-based foods during gastric digestion and its link to glycemic response: In vivo and in vitro considerations. *Comprehensive Reviews in Food Science and Food Safety, 20*(3), 2660–2698.
Nadia, J., Olenskyj, A. G., Stroebinger, N., Hodgkinson, S. M., Estevez, T. G., Subramanian, P., … Bornhorst, G. M. (2021). Tracking physical breakdown of rice- and wheat-based foods with varying structures during gastric digestion and its influence on gastric emptying in a growing pig model. *Food & Function, 12*, 4349–4372.
Nau, F., Nyemb-Diop, K., Lechevalier, V., Floury, J., Serrière, C., Stroebinger, N., … Rutherfurd, S. M. (2019). Spatial-temporal changes in pH, structure and rheology of the gastric chyme in pigs as influenced by egg white gel properties. *Food Chemistry, 280*, 210–220.
Olenskyj, A. G., Donis-González, I. R., & Bornhorst, G. M. (2020). Nondestructive characterization of structural changes during in vitro gastric digestion of apples using 3D time-series micro-computed tomography. *Journal of Food Engineering, 267*, Article 109692.
Pellegrini, N., Vittadini, E., & Fogliano, V. (2020). Designing food structure to slow down digestion in starch-rich products. *Current Opinion in Food Science, 32*, 50–57.
Ramadoss, B. R., Gangola, M. P., Agasimani, S., Jaiswal, S., Venkatesan, T., Sundaram, G. R., & Chibbar, R. N. (2019). Starch granule size and amylopectin chain length influence starch in vitro enzymatic digestibility in selected rice mutants with similar amylose concentration. *Journal of Food Science and Technology, 56*(1), 391–400.
Ranawana, V., Henry, C. J. K., & Pratt, M. (2010). Degree of habitual mastication seems to contribute to interindividual variations in the glycemic response to rice but not to spaghetti. *Nutrition Research, 30*, 382–391.
Reynolds, T. D., Mitchell, S. A., & Balwinski, K. M. (2002). Investigation of the Effect of Tablet Surface Area/Volume on Drug Release from Hydroxypropylmethylcellulose Controlled-Release Matrix Tablets. *Drug Development and Industrial Pharmacy, 28*(4), 457–466.
Siepmann, J., & Siepmann, F. (2012). Modeling of diffusion controlled drug delivery. *Journal of Controlled Release, 161*(2), 351–362.
Singh, J., Dartois, A., & Kaur, L. (2010). Starch digestibility in food matrix: A review. *Trends in Food Science & Technology, 21*, 168–180.
Singh, V., & Ali, S. Z. (2006). In vitro hydrolysis of starches by α-amylase in comparison to that by acid. *American Journal of Food Technology, 1*(1), 43–51.
Somaratne, G., Reis, M. M., Ferrua, M. J., Ye, A., Nau, F., Floury, J., … Singh, J. (2019). Mapping the Spatiotemporal Distribution of Acid and Moisture in Food Structures during Gastric Juice Diffusion Using Hyperspectral Imaging. *Journal of Agricultural and Food Chemistry, 67*(33), 9399–9410.
Somaratne, G., Ye, A., Nau, F., Ferrua, M. J., Dupont, D., Paul Singh, R., & Singh, J. (2020). Role of biochemical and mechanical disintegration on β-carotene release from steamed and fried sweet potatoes during in vitro gastric digestion. *Food Research International, 136*, Article 109481.
Swackhamer, C., Doan, R., & Bornhorst, G. M. (2022). Development and characterization of standardized model, solid foods with varying breakdown rates during gastric digestion. *Journal of Food Engineering, 316*, Article 110827.
Swackhamer, C., Zhang, Z., Taha, A. Y., & Bornhorst, G. M. (2019). Fatty acid bioaccessibility and structural breakdown from in vitro digestion of almond particles. *Food & Function, 10*(8), 5174–5187.
Tagle-Freire, D., Mennah-Govela, Y., & Bornhorst, G. M. (2022). Starch and Protein Hydrolysis in Cooked Quinoa (Chenopodium quinoa Willd.). *during Static and Dynamic In Vitro Oral and Gastric Digestion. Food & Function*.
Tamura, M., Okazaki, Y., Kumagai, C., & Ogawa, Y. (2017). The importance of an oral digestion step in evaluating simulated in vitro digestibility of starch from cooked rice grain. *Food Research International, 94*, 6–12.
Tamura, M., Singh, J., Kaur, L., & Ogawa, Y. (2016). Impact of structural characteristics on starch digestibility of cooked rice. *Food Chemistry, 191*, 91–97.
Vanhatalo, S., Dall'Asta, M., Cossu, M., Chiavaroli, L., Francinelli, V., Pede, G. D., … Scazzina, F. (2021). Pasta Structure Affects Mastication, Bolus Properties, and Postprandial Glucose and Insulin Metabolism in Healthy Adults. *The Journal of Nutrition*.
Wu, P., Deng, R., Wu, X., Wang, Y., Dong, Z., Dhital, S., & Chen, X. D. (2017). In vitro gastric digestion of cooked white and brown rice using a dynamic rat stomach model. *Food Chemistry, 237*, 1065–1072.
Zou, W., Sissons, M., Gidley, M. J., Gilbert, R. G., & Warren, F. J. (2015). Combined techniques for characterising pasta structure reveals how the gluten network slows enzymic digestion rate. *Food Chemistry, 188*, 559–568.